A palaeontological and geochemical analysis of vertebrate fossils from a Late Quaternary cave deposit in Southeastern Australia with a particular focus on bone surface coatings

Thesis submitted in accordance with the requirements of the University of Adelaide for an Honours Degree in Geology

Andrew Jeremy Chua

July 2020

THE UNIVERSITY of ADELAIDE

A PALAEONTOLOGICAL AND GEOCHEMICAL ANALYSIS OF VERTEBRATE FOSSILS FROM A LATE QUATERNARY CAVE DEPOSIT IN SOUTHEASTERN AUSTRALIA WITH A PARTICULAR FOCUS ON BONE SURFACE COATINGS

BLANCHE CAVE PALAEONTOLOGY AND GEOCHEMISTRY

ABSTRACT

The Naracoorte Caves National Park hosts many well-preserved cave fossil deposits that span the last 500 ka. The sedimentary sequences and fossil bone assemblages across over 50 sites provide insights into past climatic conditions as well as faunal responses to Pleistocene climate change, covering significant events such as the Last Glacial Maximum and the extinction of Australian megafauna. However, faunal assemblages can be easily biased by variations in accumulation mode or bone preservation. In this study, I conducted a palaeontological and taphonomic analysis on fossil bone material from an unfinished excavation in Chamber 1 of Blanche Cave, focussing on bone surface coatings to infer the post-burial conditions of the site. SEM results identified three different coatings: black coatings were manganese, white coatings were gypsum, and crystalline coatings were phosphate. Oxidation of ions by chemolithotrophic microorganisms is hypothesized to be the main mechanism for the formation of the three coatings. Bat guano also plays an important role in altering the soil environment, such as providing sulphur and phosphorus and lowering soil pH. This potentially allows for gypsum and phosphate to be used for tracing past bat activity. The study site also agrees with other synchronous sites at the NCNP (Third Chamber, Blanche Cave and Wet Cave) in terms of its sediment sequence and faunal assemblages with small variability, likely due to variations in entrance size and distance from the accumulation point. Further investigation of authigenic minerals and surface coatings is needed as there is potential for them to be used as environmental proxies. More geochronologic work is needed to more accurately place the site material in context.

KEYWORDS

Blanche Cave, Palaeontology, Geochemistry, Bone surface coatings, Manganese,

Gypsum, Phosphate, Guano

TABLE OF CONTENTS

LIST OF FIGURES AND TABLES

INTRODUCTION

The Naracoorte Caves National Park (NCNP) is an important site for Late Quaternary palaeontology. The region has over 50 cave sites with infill deposits that span the last 500 ka (Reed & Bourne, 2009). The well preserved megafaunal assemblage in some of the Late Pleistocene sites have been dated near the estimated 39-51 ka Australian megafaunal extinction window proposed by Roberts et al. (2001). This makes them important in advancing the Australian megafaunal extinction debate. Previous work at Naracoorte included palaeontological, geochronological, and taphonomic studies. These are key in understanding how fauna adapted to climate (Macken et al., 2012; Prideaux et al., 2007) and biodiversity changed over time. Critical to understanding how representative the Naracoorte deposits are to the original palaeocommunities is assessment of the site's taphonomic history and any preservational bisases present in cave deposits (Fraser & Wells, 2006; Reed, 2006).

One potential source of bias is destruction or modification of bone during diagenesis following burial in cave sediments. Bone surface coatings, while present in many deposits, have been described but not examined further in previous studies (Laslett, 2006; Reed, 2006). Some of these coatings may also lead to damage to bone and poor preservation. Dark coatings on bone have been attributed to Manganese or Iron based stains that form after burial. These coatings have been used as evidence of water pooling, as partial inundation of bone is suggested to be a requirement for the coating process. While studies on dark coatings found in other fossil sites have proven useful in determining the taphonomic history of a site (Foecke, 2016; Marín Arroyo et al., 2008;

Shahack-Gross et al., 1997), different oxides can produce similar looking coatings and proper identification of these stains is needed. There have also been white coatings found on some of the bones at Naracoorte that could be phosphate nodules. Nodules can form due to leaching of bat guano, where the dark soluble nitrate component is removed (Hill, 1982). Forbes & Bestland (2006) have identified the white nodules found in some of the deposits at Naracoorte as biogenic phosphate.

The overarching aim of this thesis is to conduct a chronostratigraphic, geochemical, and faunal analysis of Blanche Cave Chamber 1. This will be achieved via a series of specific objectives, as follows:

1. Determine the chronostratigraphic context of the fossil bone material to correlate this site with similar deposits in the NCNP.
2. Use statistical analyses to identify variability in relative abundance of different animal groups through time.
3. Geochemically identify and analyse different bone surface coatings found on the fossil material to infer the post-depositional histories of elements in the assemblage.

Fossil material from an unfinished excavation by S. Brown in 2001 (Reed, Pers. comm.) will be used. Novel methods and proxies for taphonomic research will be explored to examine their viability for corroborating and complementing current data for Blanche Cave and related sites. With all of this taken into consideration, my main hypotheses are:

1. The composition and changes in faunal succession in this study are similar to other Late Pleistocene NCNP sites.
2. Black coatings found on bones are manganese stains formed due to partial inundation of bone in water.
3. White powdery coatings are authigenic gypsum that has formed on the bone surface.
4. Crystalline coatings are new phosphate minerals growing from degraded bone that has been recrystallized.

BACKGROUND

Study Site

The Naracoorte Caves are a group of Pleistocene limestone caves located in the south eastern region of South Australia. Cave formation was estimated to have occurred in the Miocene Gambier Limestone between 0.8-1.1 Ma (White & Webb, 2015). The same study suggested that the flank margin cave features found in the caves indicates formation near the coastline, where multiple source waters with variable salinity interact to dissolve the porous limestone. Sea level regression then drained the caves completely at 780-880 ka, after which the caves opened to the surface and began to collect sediment and bone. The region has over 50 sites that range from Middle to Late Pleistocene in age, with the oldest dated at 528 ± 41 ka, and have well preserved faunal deposits (Reed & Bourne, 2009).

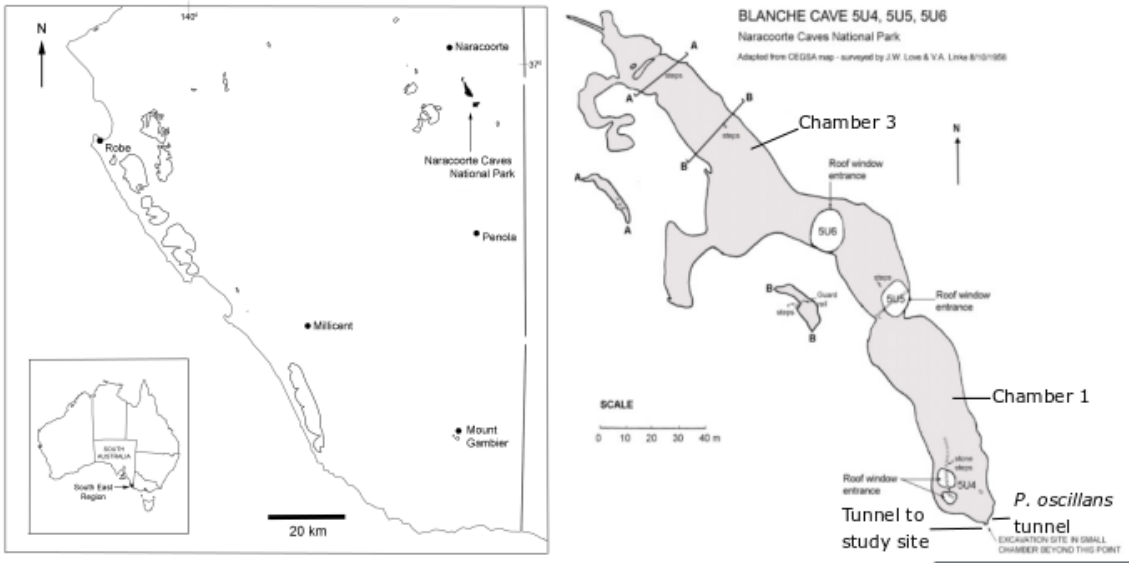

Figure 1: (a) Location of the Naracoorte Caves in the Southeastern region of South Australia. (b) Area map of Blanche Cave. The third chamber site is closest to the 5U6 roof window while the first chamber site is accessed via a small tunnel southeast of 5U4.

Some of the caves, such as Blanche and Wet cave, within the World Heritage listed Naracoorte Caves National Park, contain Late Pleistocene-Holocene deposits that capture the proposed 39-51 ka extinction window by Roberts et al. (2001). Blanche Cave, the study site for this project, has around 200 m of passage with three chambers with large open roof windows [Figure 1]. Parts of the cave are used for over-wintering by the Southern Bentwing Bat (*Miniopterus orianae basanii*). Previous palaeontological studies in Blanche cave have centred on the third chamber site, investigating its faunal, geochronological, and sedimentological characteristics (Laslett, 2006; Macken & Reed, 2013; Macken et al., 2013b). The study site for this project is located near the main chamber of Blanche Cave, and is in a small (~25 sq.m) chamber accessed by a short tunnel close to the 5U4 entrance. Another point of interest for this site is its proximity to the location where the only specimen of the large extinct bird *Genyornis newtoni* has been found (Reed and Bourne, 2000).

A preliminary study at the site was conducted by Flinders University MSc student Steve Brown in 2001 (Brown, 2006). Much of the excavated material was not processed as the project was abandoned. It has been stored at the Naracoorte Caves NP lab since 2001 and retrieved for this study. 61 bags of bulk material were also collected and labelled with the grid square and depth. Charcoal samples were collected by S. Brown from the north face of the pit, with only two of them yielding dates. The samples were carbon dated with standard acid prep and measured with an accelerated mass spectrometer.

Megafaunal extinction

Since this site is hypothesized to be contemporaneous with the third chamber dig and contains megafaunal remains, it can help advance our understanding of the extinction of Australian megafauna. The timing and causes of extinction in Australia have been debated, with a divide between climate-driven (Field et al., 2008) and anthropogenic (Gillespie et al., 2008; Saltré et al., 2016) mechanisms. While the deposits at Naracoorte have finely resolved stratigraphy and a well preserved, continuous fossil record, no evidence for human activity has been found for this time period. This allows examination of the effects of changing climate on the faunal assemblages. Site studies at Naracoorte have also produced different results, with some suggesting that mammal persistence into the Holocene shows adaptation to climate (Prideaux et al., 2007). Macken & Reed (2013), on the other hand, attributed range shifts in small mammals in three different cave deposits to climate change. However, Macken et al. (2012) stress that mammalian response to climate change varies between species and climate.

Taphonomy

Taphonomic analysis of various deposits also provided insight on the processes that governed the accumulation of bones and sediment (Fraser & Wells, 2006; Laslett, 2006; Reed, 2006). This is important for identifying biases and what is missing from a fossil assemblage. For example, solution pipe entrances are small, almost vertical holes at the roof of the cave. The main mode of accumulation would then be animals falling into the hole, limiting the maximum size to whatever can fit in the hole, as well as not discriminating between age groups. Examples of this type of deposit would be Grant Hall (Fraser & Wells, 2006) and the Ossuaries (Reed, 2006). Reed (2006) also hypothesized a possible bias of these entrances towards mode of locomotion due to the higher abundance of saltatorial animals, as well as noting that there was a greater proportion of articulated specimens further away from the sediment cone near the entrance. This suggested that the animals must have survived the fall and explored the cave, trampling the bones near the entrance, and then settling near the cave walls. Analysis of the third Chamber deposit in Blanche Cave revealed large animal remains with trample marks and a dense collection of smaller mammals with acid etched bone surfaces, which was interpreted as a combination of pitfall and owls as the main accumulation modes (Laslett, 2006). Owls can hunt and consume small mammals and prefer to roost in open caves, regurgitating prey bones as pellets on the cave floor. This creates a bias towards high numbers of prey with slightly damaged bones due to the stomach acid of the owl. Understanding these systematic biases provides a better picture of the faunal assemblage of each deposit.

Bone Surface Coatings

Bone surface coatings have been relatively unstudied at Naracoorte but there have been studies in other archaeological sites (Foecke, 2016; López-González et al., 2006;

Shahack-Gross et al., 2004). Most of these studies have focused on stained black bones, which have been originally attributed to burning (Shahack-Gross et al., 1997). However, more recent studies have found that black staining does not immediately indicate burning, and other mechanisms can stain a bone black (Fernández-Jalvo et al., 2019). The main hypothesis for the current study is that manganese stains form due to accumulation of mobile manganese ions which then enter bone and oxidize (Marín Arroyo et al., 2008). This type of coating is present in multiple cave deposits (Carmichael & Brauer, 2015; Kotula et al., 2018), providing evidence for pooling of water as it would require partial inundation of bone. Bacterial action has also been linked to these stains as a catalyst for the mobilization of manganese via oxidation during biological processes (Papier et al., 2011; Strathopolou et al., 2019).

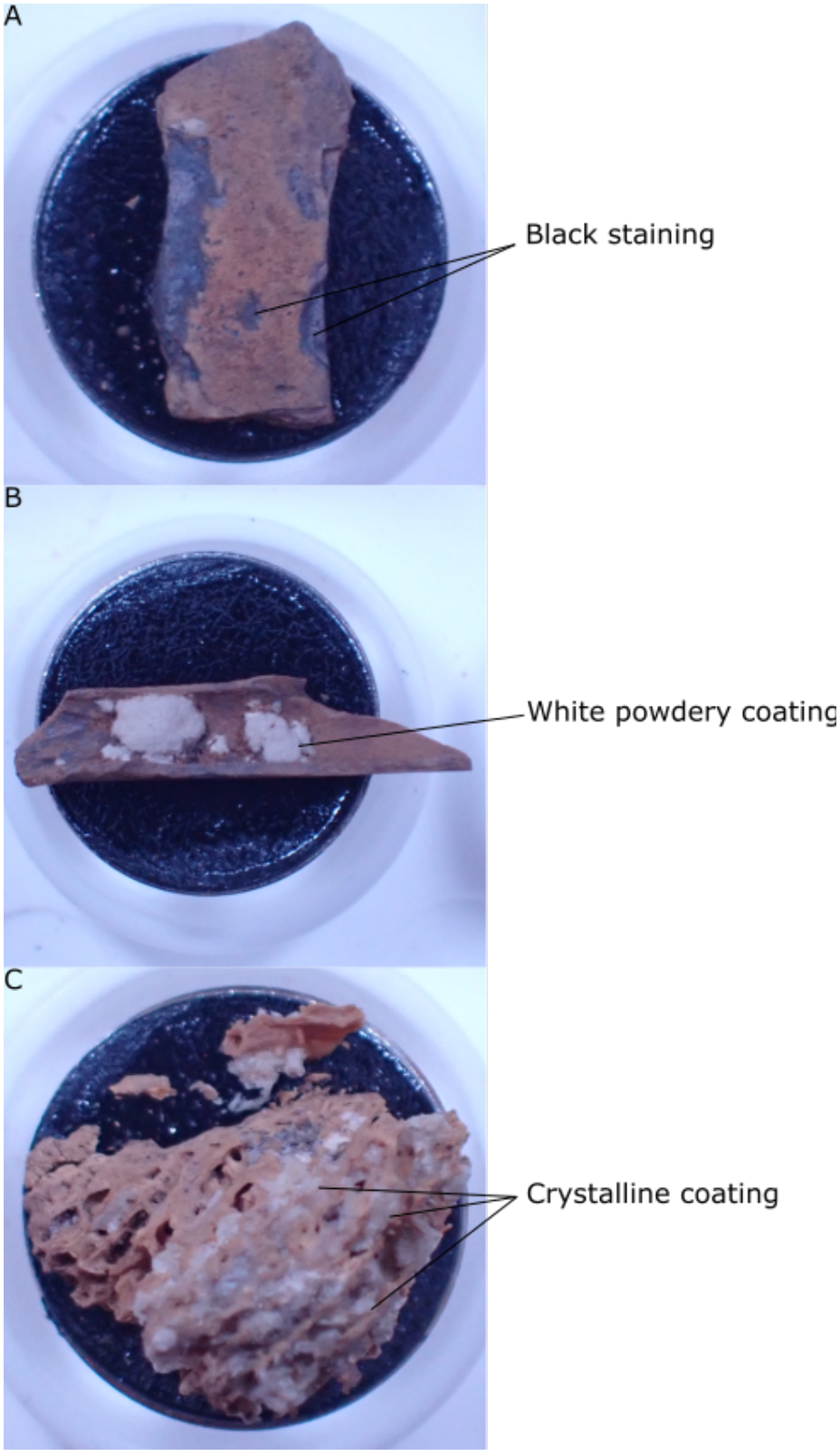

Figure 2: Different surface coatings found on bone fragments used for SEM analysis. (a) Sample Mn_3 is a fragment of cortical bone with black stains hypothesized to be manganese coats. (b) S_1 is a long bone fragment of a small mammal with white powdery coatings o on the interior surface. (c) C_1 is a fragment of spongy bone with very extensive crystalline coating.

The white powdery material [Figure 2] has not been studied or recorded on bone at Naracoorte, but Laslett (2006) note the presence of similar white nodules in the sediment of one unit of Blanche Cave, which was geochemically identified in the chamber 1 site as guano-derived phosphate (Forbes & Bestland, 2006). Another white mineral that has appeared in older Naracoorte units is gypsum (Darrénougué et al., 2009) but it has only been mentioned in passing as weak evidence for a cool palaeoclimate. Sulphur required to form gypsum can come from inorganic (Yonge & Krouse, 1987) or organic (Dumitras et al., 2008; Snow et al., 2014) sources.

The crystalline coating appears to have a more destructive effect on bone, making some elements unidentifiable. Shahack-Gross et al. (2004) studied the effects of bat guano on bone preservation and show that decomposing guano creates changes in pH which degrade bone material and promote growth of different authigenic mineral assemblages. Water entering the cave would incorporate carbonates from the limestone and buffer the pH, preserving the bone. Degrading guano can produce multiple assemblages of minerals, including gypsum and apatite, depending on the environmental conditions (Audra et al., 2019).

Understanding how these coatings form is important in understanding depositional conditions and soil environments that must have occurred to help reconstruct a sequence of events from burial to excavation (Hollund et al., 2018; Shahack-Gross et al., 2004). However, it is difficult to use coatings as a proxy for large-scale palaeoclimate changes as the microenvironments that promotes their mineralization can be very localized on scales of centimetres or meters (Karkanas et al. 2000).

METHODS

Sedimentology and Geochronology

Field work for this study included taking pictures, drawing a plan view of the chamber, transects, a stratigraphic section, and collecting sediment samples. A Leica Disto laser rangefinder was used to measure the plan view and both transverse sections of the cave. The floor was not measured since the pit has been dug and measuring the original sediment surface would be impossible. The latitudinal transect selected was roughly perpendicular to the longitudinal section and best displayed the ceiling features. Stratigraphic sections were drawn for the north and east faces of the pit, as these two walls best represent the sedimentary sequence.

A total of 16 samples (in 70 ml vials) were collected from six sedimentary units for geochemical analysis and comparison (Appendix A). One sample was taken from overburden for visual comparison. Eight samples (one from each unit) were sent to Bureau Veritas for XRF bulk geochemistry. Three partially filled vials of large white nodules and one vial of scraped white material were collected from Unit 1 for qualitative XRD. XRD procedures and specifications can be found in Appendix B.

Faunal Succession

For the current study, bulk material from grid square 4 was then wet sieved to remove sediment from the bone surfaces and then sorted. This process is outlined in Appendix C. The box and sorted bulk material were then catalogued, noting the presence of bone coatings and other taphonomic features. Faunal identification was completed using comparative material and relevant literature, including material from the South

Australian Museum (SAM) palaeontology collection. A series of palaeontological statistical analyses were used to determine the composition and change of faunal assemblages in the site.

Number of Identified Specimens (NISP) was used to estimate the frequency of identifiable fossils for the fauna from the site. Specimens were counted based on cranial elements only for each depth or stratigraphic unit. Since each identifiable element is considered as one individual, NISP tends to overestimate populations, especially in heavily fractured assemblages. Relative Abundance (RA%) is used to reduce the overestimation of NISP by calculating the proportions of a group relative to the total number of individuals in that depth or stratigraphic unit. This reduces taphonomic and sampling biases when analysing relationships between groups. For this study, the Minimum Number of Individuals (MNI) was calculated for cranial specimens by counting the number of left and right maxillae and dentaries of a group and selecting the most abundant element. MNI can lead to underrepresentation of populations since individuals can have only one element preserved. In some cases, whole groups are missing since they are not represented in the assemblage by their maxillae or dentaries.

Surface Coatings

SEM-EDS

Five fossil bone fragments (Appendix D) were selected for SEM-EDS analysis to determine the elemental composition of the coatings. The fragments were selected based on the size and quality of their surface coatings. Three samples were analysed for the black coating, one for the powdery white coating, and one for the crystalline coating.

Samples were first heated in an oven at 40C to remove any remaining moisture in the bone. These were then sent to Adelaide Microscopy (AM) for coating and analysis with using a FEI Quanta 450 with standard settings (HV = 10.0 kv, beam diameter = 2.5). The samples were platinum coated by AM staff to produce clearer SEM images. While only producing qualitative data, the SEM-EDS detects relative abundances of elements on the surface of the bone, which is enough for identifying the main components of the coatings.

NISP AND RA

NISP and RA% was also conducted on the bone surface coatings to see variations in the extent of different coatings with depth. Each specimen number that had a coating was counted as one individual. A specimen can have multiple types of coatings and would then be considered as one individual for each of those types. The abundance and extent of the coating did not affect the count.

THIN SECTION

Three samples of bone were sent to Adelaide Petrography to have thin sections cut to determine the extent of destruction found in bones with white crystalline coatings. The samples were chosen to represent different stages in the bone coating process for the crystalline material, one without coatings (as ‘control’), one with coatings on the surface and one that was so coated the bone structure was compromised. Samples were encased in epoxy resin before being cut. Images were taken using an Olympus BX51 microscope using transmitted light.

OBSERVATIONS AND RESULTS

Sedimentology and Geochronology

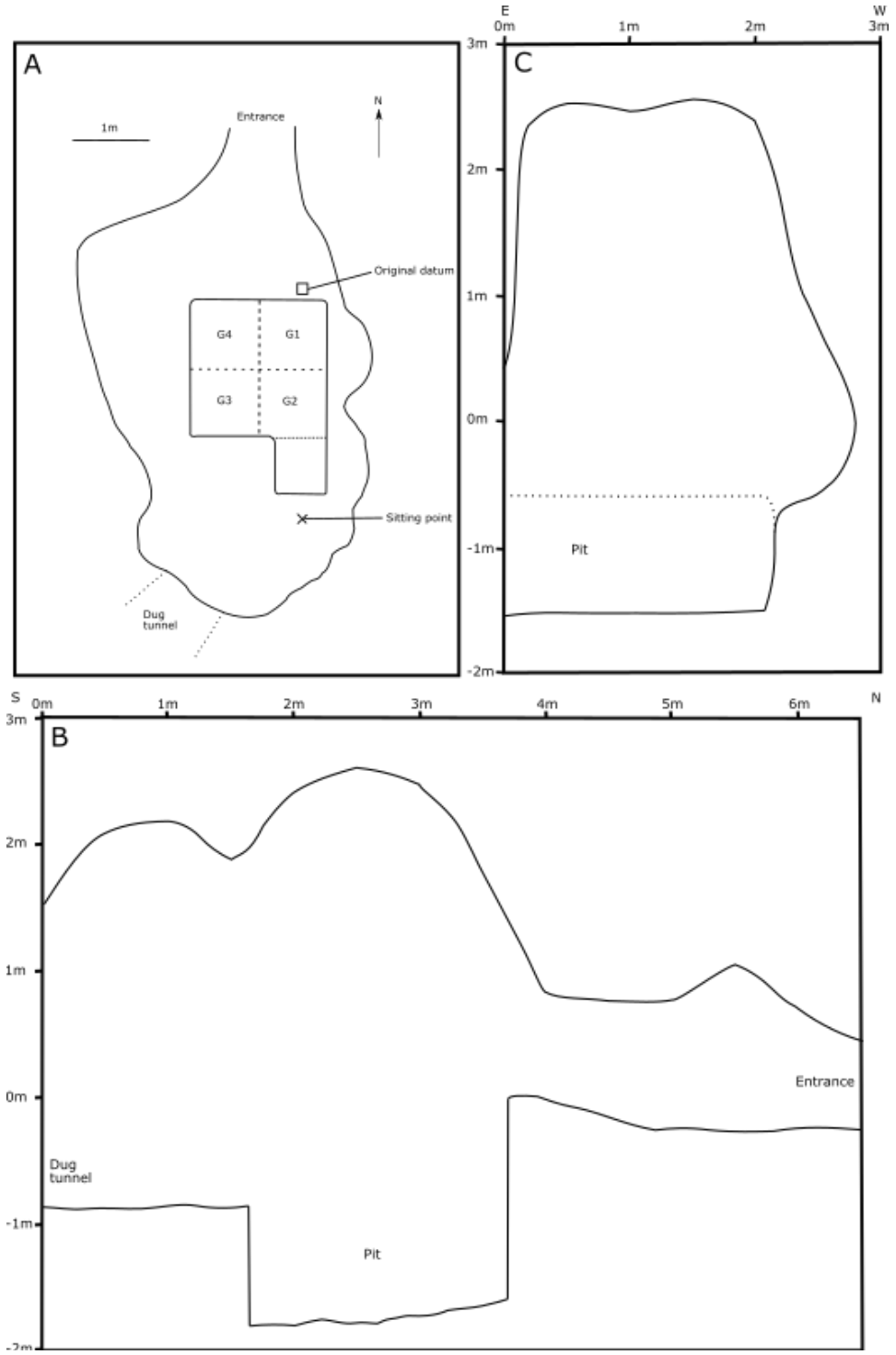

Figure 3: Rough diagrams of the (a) plan view, (b) longitudinal section and (c) latitudinal section of the chamber. The pit itself was roughly 1.8m by 1.8m with a small 'step' dug for easy access. A small tunnel to the southwest was dug by cavers.

A total of six stratigraphic units were identified based on visual analyses of the north and east faces of the pit [Figure 3]. Sections were measured from the highest point of the overburden (disturbed sediment) until the pit floor. Since the surface height of the overburden varies, the depth of each unit will be based on the left half of the north face. Only the first three units are found in both faces. Fossil material has been recovered from Units 1-4 and the overburden. Except for the cut and fill structure on the north face, all units are relatively undisturbed and lie almost horizontally.

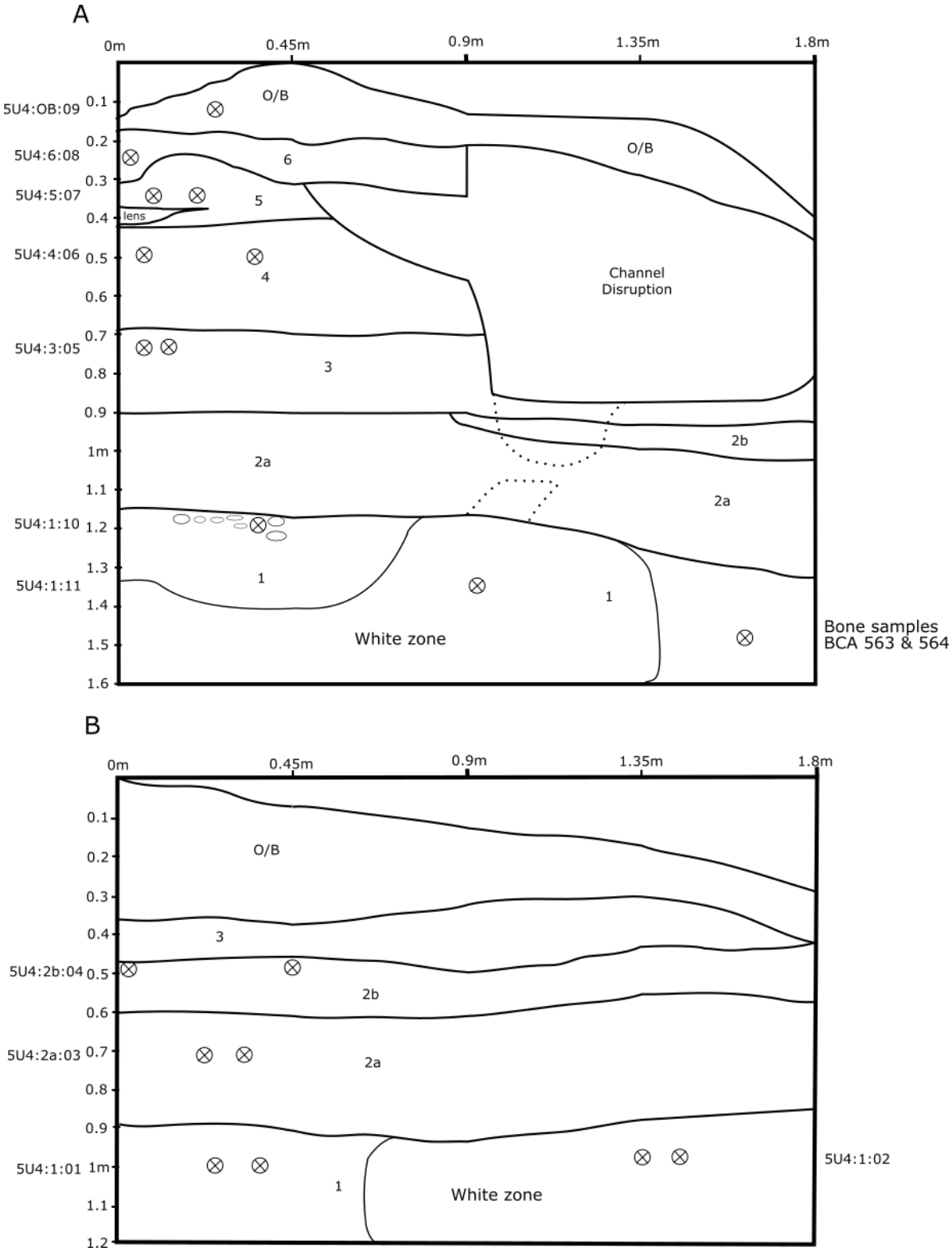

Figure 4: Stratigraphic section of the (a) north and (b) east walls of the pit. Samples were recovered from the walls at the marked locations. White zones indicate regions of sediment with incorporated white material. Carbon dates from the 2001 study were recalibr recalibrated with OxCal 4.3 using a SHCal 13 calibration curve.

Table 1: Bulk major element geochemistry of the different sediment samples collected. The naming scheme for the samples is (entrance):(unit):(sample number). Loss on ignition (LOI) is the percentage of mass lost after the sample has been heated and is used interpreted as the amount of organic matter.

Sample	UNITS	5U4:1:01	5U4:1:02	5U4:2a:03	5U4:2b:04	5U4:3:05	5U4:4:06	5U4:5:07	5U4:6:08
SiO2	%	72.11	51.24	79.03	58.76	60.23	81.79	74.76	60.34
Al2O3	%	6.69	6.49	3.63	9.85	10.01	2.62	4.01	3.38
Fe2O3	%	3.68	3.73	1.96	4.81	4.65	1.37	2.02	1.67
MnO	%	0.02	0.02	0.01	0.04	0.04	0.01	0.02	0.02
CaO	%	4.9	12.24	6	7.03	5.26	5.54	6.03	11.25
MgO	%	0.42	0.55	0.54	1.72	1.63	0.52	1.23	1.3
K2O	%	0.625	0.602	0.503	1.35	1.42	0.45	0.609	0.494
Na2O	%	0.79	0.95	0.48	1.37	0.95	0.31	0.39	0.44
P2O5	%	3.19	3.6	0.334	0.349	0.401	0.139	0.313	0.714
SO3	%	0.26	9.59	0.19	0.36	0.17	0.12	0.61	5.78
TiO2	%	0.38	0.35	0.26	0.6	0.69	0.21	0.28	0.24
V2O5	%	0.01	0.009	0.005	0.013	0.013	0.003	0.005	0.004
Cr2O3	%	0.008	0.007	0.005	0.007	0.008	0.003	0.005	0.002
BaO	%	0.018	0.02	0.012	0.02	0.022	0.008	0.011	0.012
NiO	%	0.002	0.003	-0.001	0.002	0.002	-0.001	-0.001	-0.001
CuO	%	0.002	0.003	0.002	0.003	0.004	0.002	0.002	0.002
Co3O4	%	-0.001	0.001	-0.001	-0.001	-0.001	-0.001	-0.001	-0.001
PbO	%	-0.001	-0.001	-0.001	-0.001	-0.001	-0.001	-0.001	-0.001
ZnO	%	0.01	0.012	0.002	0.003	0.004	-0.001	0.002	0.002
As2O3	%	0.002	0.002	0.002	0.002	0.002	-0.001	-0.001	0.002
SnO2	%	-0.001	0.002	-0.001	-0.001	-0.001	-0.001	-0.001	0.002
SrO	%	0.014	0.019	0.007	0.012	0.016	0.01	0.013	0.018
ZrO2	%	0.021	0.013	0.015	0.024	0.024	0.013	0.016	0.014
Cl	%	0.644	1.09	0.426	1.42	0.904	0.323	0.543	0.76
LOI1000	%	6.68	13.2	6.86	13.5	14.2	6.9	9.62	17.9

Unit 1 (-115cm to -160cm) is a very dark red-brown clayey sand layer that contains regions with white powdery material and larger (cm scale) white nodules. The unit is densely packed and is sticky to the touch, suggesting a high clay content. There is a ~70 cm wide bowl-shaped structure on the north face which marks a boundary between regions with and without white powdery material [Figure 4]. While this same material is seen on the pit surface of the uppermost units (5, 6, overburden), it is only well incorporated in Unit 1. The regions of sediment with white material appear to be patchy and are not uniform throughout the unit. Bulk geochemistry of these regions have higher SO3 (9.59%) than average (>1%). The unit also contains elevated P2O5 (3.1-3.6%) compared to all other units (>1%) [Table 1].

Unit 2 (-90cm to -115cm) consists of lighter red-brown clay sands that contain very thin (up to 20mm) lenses of light brown quartz sand. The laminations are very clear on the east face, but are more discontinuous on the north face, which is more disrupted [Figure 4]. The boundary at the base of this unit is gradational, with the key differences being texture and colour. The base of this layer has some megafaunal material. A roughly 10 cm thick subunit (Unit 2b) is present in the east face and continues on the north wall but pinches off halfway through the wall. This subunit is the same brown coloured clay but without the interbedded light brown quartz sands. There are small patches of incorporated white material in this unit as well (noted by the dotted lines) [Figure 4].

Unit 3 (-70cm to -90cm) is a brown coloured, undifferentiated clayey fine sand to silt layer that pinches out on the eastern side of the east face as it is covered by overburden [Figure 4]. The main characteristic of this unit is its extremely soft and sticky texture, which is used to determine the boundary between this unit and Unit 2b. The upper boundary of this unit is defined by the change to a lighter colour in the sediment. Parts of this layer are also cut through by the channel structure, and a portion of this unit just below the cut has incorporated white material within it.

Like Unit 2a, Unit 4 (-40cm to -70cm) also has interbedded centimetre-scale layers of light brown sand and brown clay silt. However, Unit 4 does not have a reddish colour, contains more quartz sand in more consistent laminated layers, and bits of charcoal. This layer has been carbon dated in the original study and recalibrated here to 15,524 - 16,277 cal yr BP.

Unit 5 (-30cm to -40cm) is a soft, dark brown clayey fine sand layer with a texture like unit 3. There is a ~5 cm thick dark lens at the base of the layer that thins to the east, presumed to have formed from possum scat. It also contains one thin (~1 cm) layer of light brown coarser sand material. The unit is cut off by the cut and fill structure associated with the channel. The upper boundary of this unit also looks to have been cut on the western edge of the north wall by unit 6 and is more irregular than all of the others. Charcoal was sampled at this boundary in the original study, with a recalibrated age of 12,074 - 12,685 cal yr BP, which is just at the start of the Holocene.

Unit 6 (-18cm to -30cm) is a loosely packed, dull, light grey clay sand layer that contains fragments of white material. While similar in colour to the powdery nodules in Unit 1, the material is more comparable to carbonate. Like Unit 5, this unit is only seen in the left half of the north face, cut off by the channel disruption. The upper boundary is distinct as the colour of the overburden is reddish-brown.

Faunal Succession

Since the depths recorded by S. Brown did not indicate the point in the cave where he measured from, I attempted to correlate the 10 cm intervals with the units found in the pit. The most logical possibility is that the depths were with respect to the level of the sediment floor without counting overburden. This was based on colour matching between bones and sediment, as well as the fact that megafauna only appeared in the Third Chamber pit at the dark reddish clay Unit 1 (Laslett, 2006). Based on this, Unit 1 would correspond to 60-100cm, Unit 2a is 40-60cm, Unit 2b is 30-40cm, Unit 3 is 20-30cm, with Unit 4 being 0-20cm. Since the original sediment surface was different for

different grid squares, there may have been some Holocene material (Unit 5-6) classed as 0-10cm or overburden.

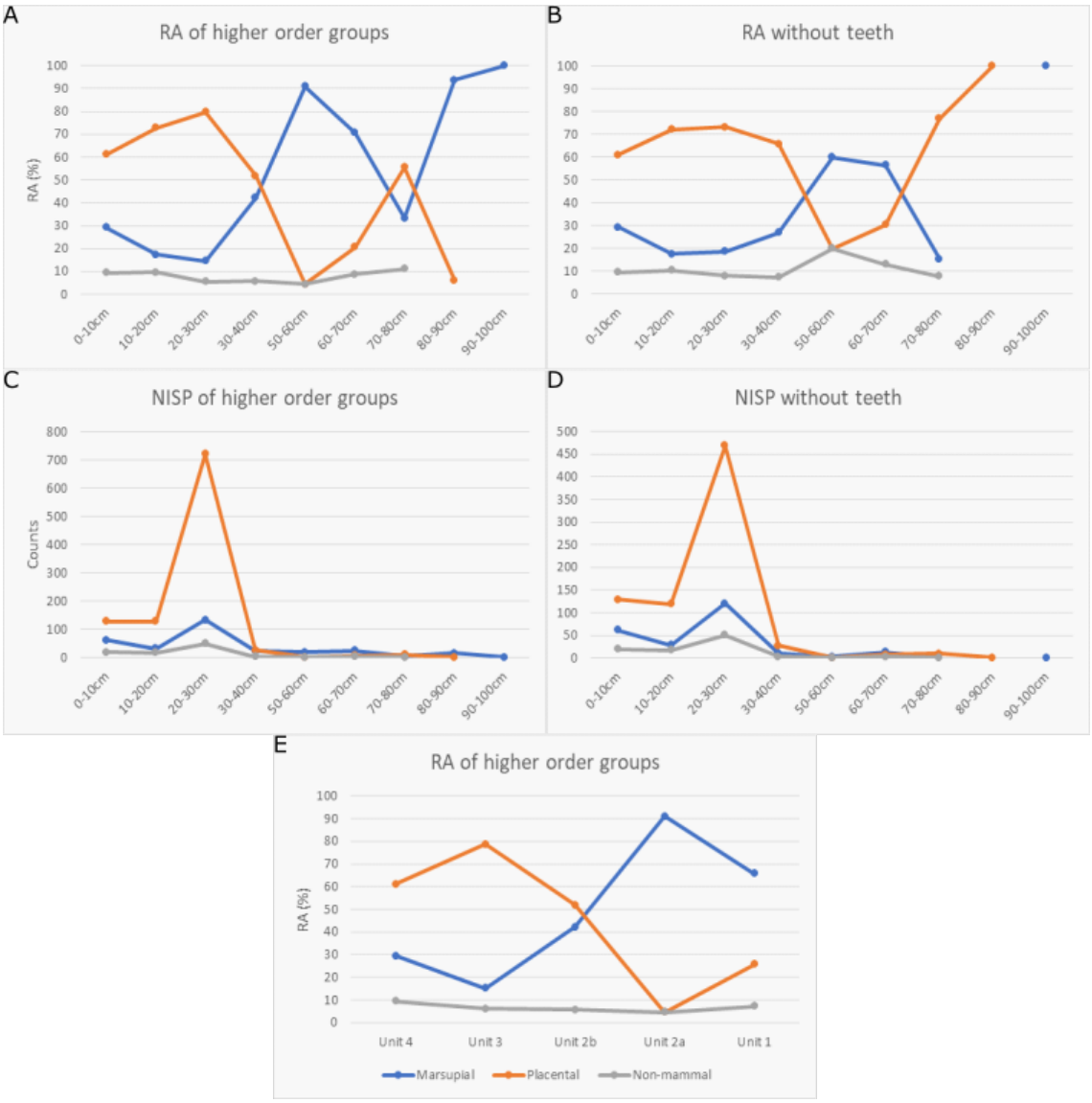

Figure 5: RA% and NISP of higher groups (marsupial, placental, non-mammal) (a, c) with and (b, d) without counting tooth elements. (e) RA% of these groups (counting teeth) based on sedimentary unit instead of depth.

Between the major groups of animals (marsupial, placental, reptile), placentals dominate the assemblage (67.91%) especially in the upper units with a large peak of 641 counts at 20-30cm [Figure 5]. This is followed by marsupials (23.21%) with reptiles (7.07%) being the least common. Avian bones were found during sorting of bulk material but were not included since they were even less common than reptiles.

This pattern is still present when loose teeth were not included in the count [Figure 5]. Similarly, the relative abundances of the different groups do not change regardless if loose teeth were in the NISP [Figure 5]. The RA shows a shift from a marsupial to placental dominated fauna at 30-40cm. RA of non-mammals appear to be almost linear, staying at around 10% of the assemblage at all depths.

Table 2: Complete faunal list of all identified species in this study. 'X' marks presence in unit regardless of element. For this study, megafaunal species are considered as species that went extinct during the Pleistocene.

Species	O/B	Unit 4	Unit 3	Unit 2b	Unit 2a	Unit 1
AMPHIBIA						
ANURA			x			x
REPTILIA						
SQUAMATA						
Agamidae			x			x
Scincidae		x	x	x		x
Varanidae						x
Elapidae			x		x	x
MAMMALIA						
MARSUPIALIA						
Dasyuromorphia						
Dasyuridae	x	x	x	x	x	x
Antechinus sp. indet.						x
Dasyurus maculatus				x		
Dasyurus viverinnus						x
Dasyurus sp. indet.			x		x	x
Sarcophilus harrisii	x			x		
Sarcophilus sp. cf. S. laniarius[+]						x
Sminthopsis sp. indet.						x
Peramelemorphia						
Peramelidae	x		x	x		x
Perameles gunnii			x			
Perameles notina			x			
Diprotodontia						
Vombatidae						
Vombatus ursinus	x	x	x	x	x	x
Thylacoleonidae						
Thylacoleo carnifex[+]					x	x
Phalangeridae						
Trichosurus vulpecula					x	
Hypsiprymnodontidae						

Species	O/B	Unit 4	Unit 3	Unit 2b	Unit 2a	Unit 1
Propleopus oscillans[+]					x	
Potoroidae						
Bettongia sp. indet.	x	x	x			
Macropodidae						
Sthenurinae[+]	x				x	x
'Procoptodon' browneorum[+]					x	x
'Procoptodon' sp. cf. P. gilli[+]						x
Macropodinae						
Macropus fuliginosus[#]	x			x	x	x
Macropus sp. indet.	x	x	x			
Notomacropus greyi[+]				x		
Notomacropus rufogriseus	x				x	
Protemnodon sp. cf. *P. roechus*[+]	x			x	x	x
Burramyidae						
Cercartetus concinnus		x				
Cercartetus lepidus		x				
Cercartetus sp. indet.		x	x			
PLACENTALIA						
Chiroptera						
Vespertilionidae						
Miniopterus orianae bassani			x			x
Rodentia						
Muridae						
Mastacomys fuscus		x	x			
Notomys mitchellii	x	x	x			
*Pseudomys apodemoides**	x	x	x	x		x
Pseudomys auritus	x	x	x	x	x	x
Pseudomys australis^	x	x	x			x
Pseudomys fumeus						x
Pseudomys gouldii^	x	x	x	x		x
Pseudomys shortridgei	x	x	x	x		x
Rattus tunneyi	x					
Megafaunal Species	2			2	4	5
Total Number of Species	17	15	21	13	13	26

[+]Indicates species extinct during the Pleistocene. [#]Specimens were identified as *M. fuliginosus* as it is difficult to distinguish between *M. fuliginosus* and *M. giganteus* from cranial remains. Furthermore, a study by Easton (2006) showed that only one species of kangaroo was present at Victoria Fossil Cave, bearing more similarities to *M. fuliginosus* than *M. giganteus.* *Some specimens were not able to be identified between *P. apodemoides* and *P. novaehollandiae* due to fragmentary remains. ^Some specimens were not able to be identified between *P. australis* and *P. gouldii* due to fragmentary remains.

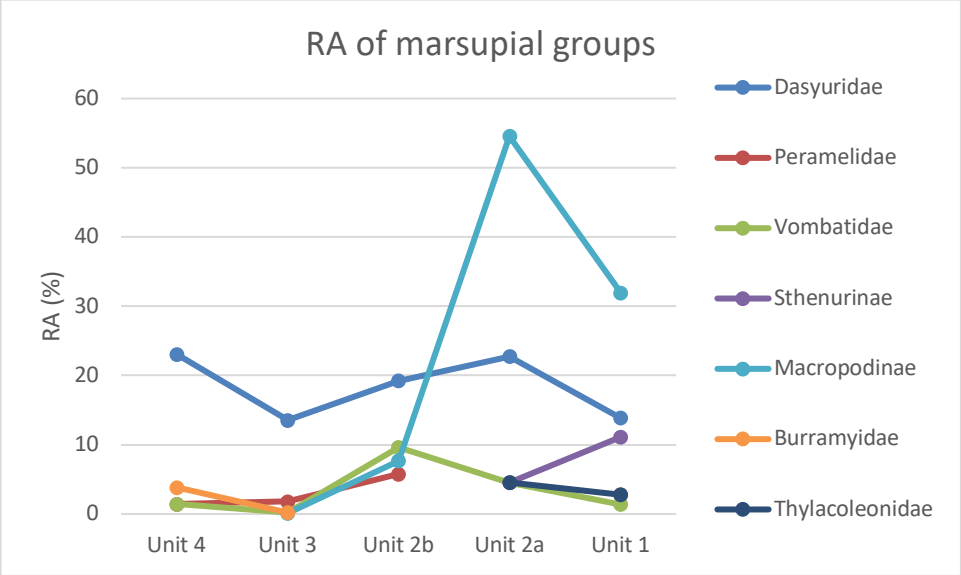

Figure 6: Relative abundances of different marsupial groups through time. Dasyuridae, Macropodinae, Thylacoleonidae and Sthenurinae had members that went extinct during the Pleistocene.

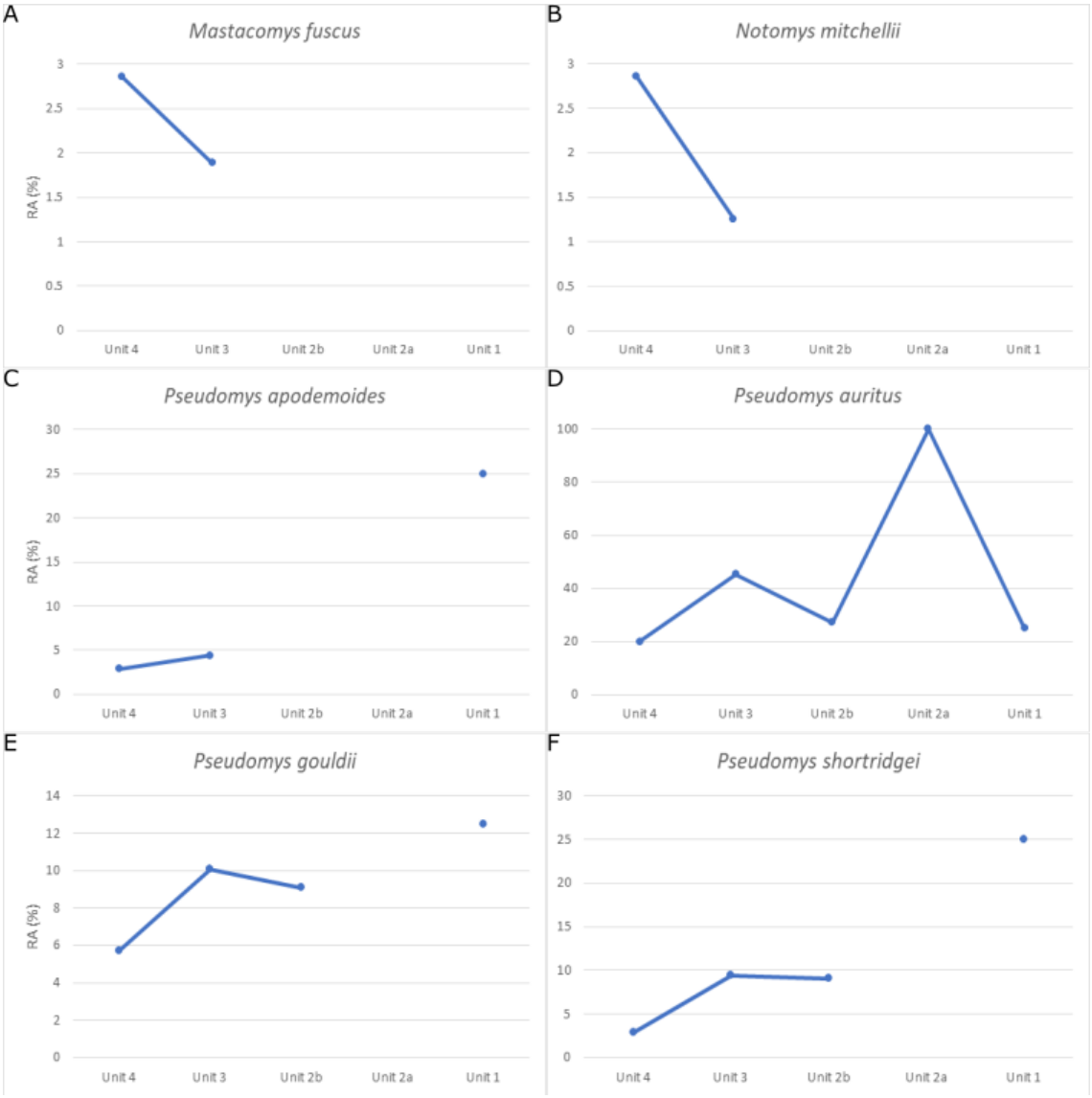

Figure 7: RA% of different Muridae species from Blanche Cave Chamber 1 calculated using their MNI showing different trends of faunal succession. (a, b) Trend 1, increase in abundance from Unit 3 to Unit 4. (c) Trend 2, relatively little change from Unit 3 to Unit 4. (d, e, f) Trend 3, decrease in abundance from Unit 3 to Unit 4.

The different megafaunal groups present in the site do not appear anywhere past Unit 2a [Table 2]. The Macropodinae, of which *Protemnodon* is a part of, show a significant decrease from 2a to 2b [Figure 6]. The other two groups that appear through the entire sequence (Dasyuridae & Vombatidae), do not show a significant change in their abundance across this boundary. The Muridae groups show 3 different patterns of succession from Unit 3 onward. Trend 1 is an increase in abundance from Unit 3 to Unit

4 [Figure 7]. Trend 2 shows relatively no change from Unit 3 to 4. The most common trend, shared across three different species, is a decrease from Unit 3 to 4.

Table 3: Occurrence of various mammals for (a) Late Pleistocene (<50 ka) sites at NCNP (Both Blanche Cave chambers (B1 & B3), Wet Cave (WC) and Robertson Cave(RC)), (b) Middle-Late Pleistocene sites at NCNP (Cathedral Cave (CC) and Grant Hall, Victoria Fossil Cave (GH)) (Reed and Bourne, 2009; Macken & Reed, 2013) and (c) mid-late Pleistocene sites from the Manning Karst Region, New South Wales (MKR) (Price et al., 2019) . 'X' marks occurrence at that site.

Family	Species	B1	B3	WC	RC	CC	GH	MKR
Tachyglossidae	*Tachyglossus aculeatus*				X	X	X	X
Thylacinidae	*Thylacinus cynocephalus*		X			X	X	
Dasyuridae	*Antechinus agilis*		X	X	X	X		
	Antechinus flavipes		X	X	X	X	X	X
	Antechinus minimus					X		
	Antechinus swainsonii					X		
	Antechinus sp. indet.	X						
	Dasyurus maculatus	X	X		X	X		
	Dasyurus viverrinus	X	X	X	X	X	X	
	Dasyurus sp. indet.	X		X	X			
	Ningaui yvonneae		X	X	X	X		
	Phascogale calura			X	X	X		
	Phascogale tapoatafa		X	X	X	X	X	
	Sarcophilus harrisii	X						X
	Sarcophilus laniarius	X		X		X		X
	Sminthopsis crassicaudata		X	X	X	X	X	
	Sminthopsis murina		X	X	X	X	X	
	Sminthopsis sp. indet.	X	X	X	X			
Peramelidae	*Isoodon obesulus*		X	X	X	X		X
	Perameles bougainville		X	X	X	X	X	
	Perameles gunnii	X	X	X	X	X	X	
	Perameles notina	X						
Phascolarctidae	*Phascolarctos cinereus*						X	
	Phascolarctos stirtoni					X		X
Diprotodontidae	*Zygomaturus trilobus*					X	X	
Palorchestidae	*Palorchestes azael*					X		
Vombatidae	Vombatidae gen. et. sp. indet.					X		
	Lasiorhinus krefftii					X		
	Vombatus ursinus	X		X		X	X	
Thylacoleonidae	*Thylacoleo carnifex*	X			X	X	X	X
Phalangeridae	*Trichosurus vulpecula*	X	X	X	X	X		X
Hypsiprymnodontidae	*Propleopus oscillans*	X						
Potoroidae	*Bettongia gaimardi*			X	X	X		X
	Bettongia lesueur		X	X	X			
	Bettongia penicillata		X			X		
	Bettongia sp. indet.	X			X			

Family	Species	B1	B3	WC	RC	CC	GH	MKR
	Potorous platyops		X	X	X	X	X	
	Potorous tridactylus		X	X	X	X	X	
Macropodidae	*Lagorchestes leporides*		X	X	X	X		
	Macropus fuliginosus	X		X	X			
	Macropus giganteus		X			X		X
	Macropus titan							X
	Macropus sp. indet.	X			X			
	Metasthenurus newtonae					X		
	Notomacropus greyi	X				X		
	Notomacropus rufogriseus	X	X			X	X	X
	Onychogalea lunata					X		
	Petrogale penicillata							X
	'Procoptodon' browneorum	X	X			X	X	
	'Procoptodon' gilli	X	X		X	X	X	
	'Procoptodon' goliah					X		
	Protemnodon brehus		X	X		X	X	
	Protemnodon roechus	X						
	Protemnodon sp. indet.			X				
	Simosthenurus maddocki					X	X	
	Simosthenurus occidentalis					X	X	
	Simosthenurus pales					X		
	Sthenurus andersoni		X			X	X	
	Sthenurinae sp. indet.			X				
	Wallabia bicolor				X	X	X	X
Acrobatidae	*Acrobates pygmaeus*		X	X	X	X		
Burramyidae	*Cercartetus concinnus*	X						
	Cercartetus lepidus	X	X	X	X	X		
	Cercartetus nanus		X	X	X	X	X	
	Cercarterus sp. indet.	X						
Pseudocheiridae	*Pseudocheirus peregrinus*		X	X	X	X	X	
Petauridae	*Petaurus breviceps*		X	X	X	X	X	
	Petaurus norfolcensis		X	X	X			
Vespertilionidae	*Miniopterus orianae bassani*	X			X		X	
	Vespertilionidae Gen et sp. indet.		X					
Muridae	*Conilurus albipes*		X	X	X	X		X
	Hydromys chrysogaster		X	X		X	X	
	Mastacomys fuscus	X	X	X	X	X	X	
	Notomys mitchelli	X	X	X	X	X	X	
	Pseudomys apodemoides	X	X	X	X	X	X	
	Pseudomys auritus	X	X	X	X	X	X	
	Pseudomys australis	X	X	X	X	X	X	
	Pseudomys fumeus	X	X	X	X	X	X	
	Pseudomys gracilicaudatus							X

Family	Species	B1	B3	WC	RC	CC	GH	MKR
	Pseudomys gouldii	X	X	X	X	X		
	Pseudomys novaehollandiae			X	X			
	Pseudomys oralis							X
	Pseudomys shortridgei	X	X	X	X	X	X	
	Pseudomys sp. indet.	X	X		X			
	Rattus fuscipes		X	X		X	X	
	Rattus lutreolus		X	X	X	X	X	
	Rattus tunneyi	X	X	X	X	X	X	
	Rattus sp. indet.			X	X			X

The study site shares 54% of its mammal species with the Third Chamber dig, and 74% with three other Late-Pleistocene to Holocene sites and NCNP [Table 3]. 80% of mammal species at the site were found in other caves at the NCNP while only 14% of its species are present in similarly aged sites (mid-late Pleistocene) in the Manning Karst Region, New South Wales. *Propleopus oscillans*, *Protemnodon roechus*, and *Cercartetus concinnus* are present in Chamber 1 but not in any of the other sites.

Surface Coatings

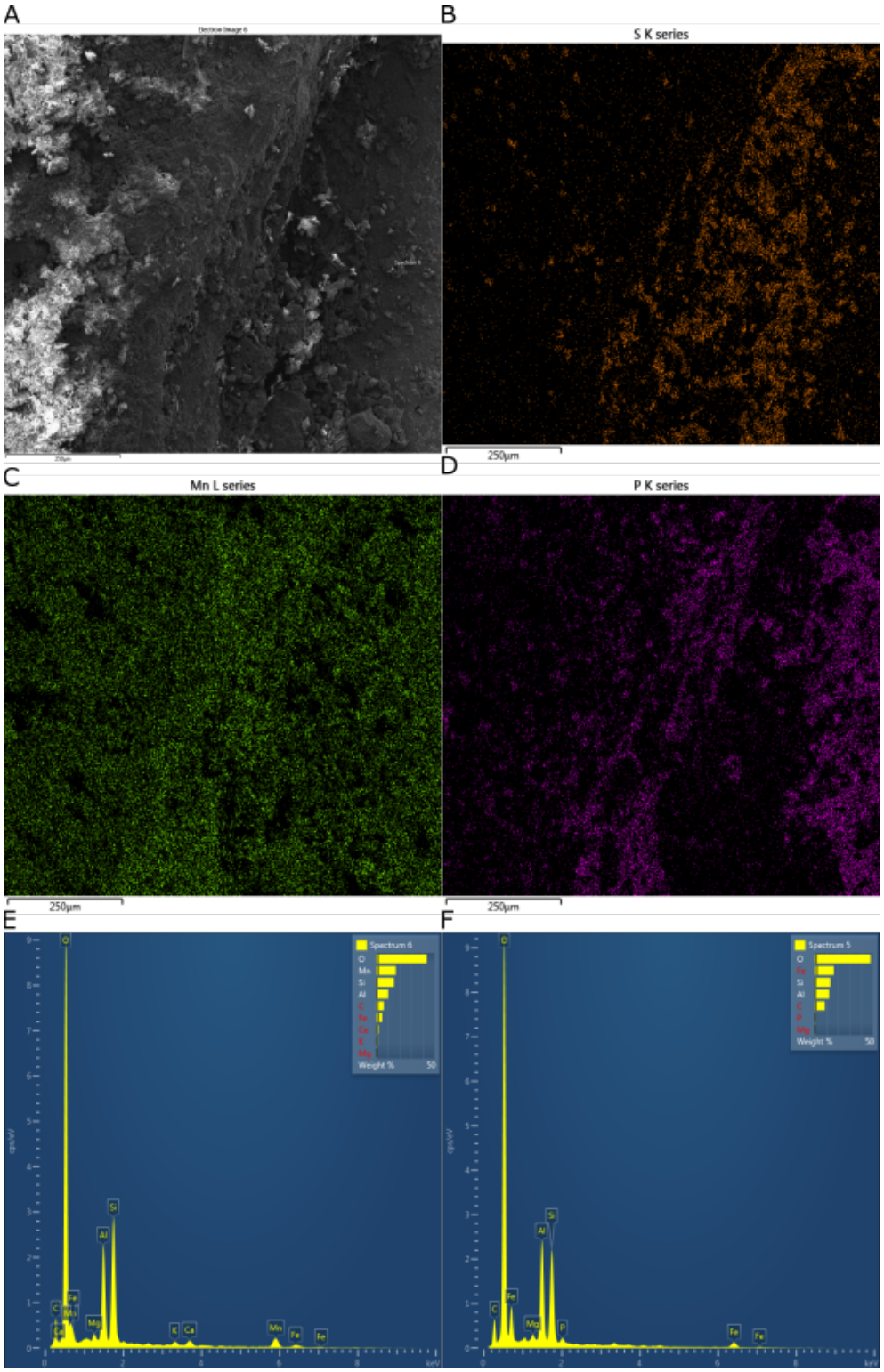

Figure 8: (a) Close up SEM image of the black coating on sample Mn_3. The portion to the right of the ridge is visually coated in black. (b, c, d) EDS elemental maps for S, Mn and P. (e, f) Elemental spectra for points annotated in the SEM image.

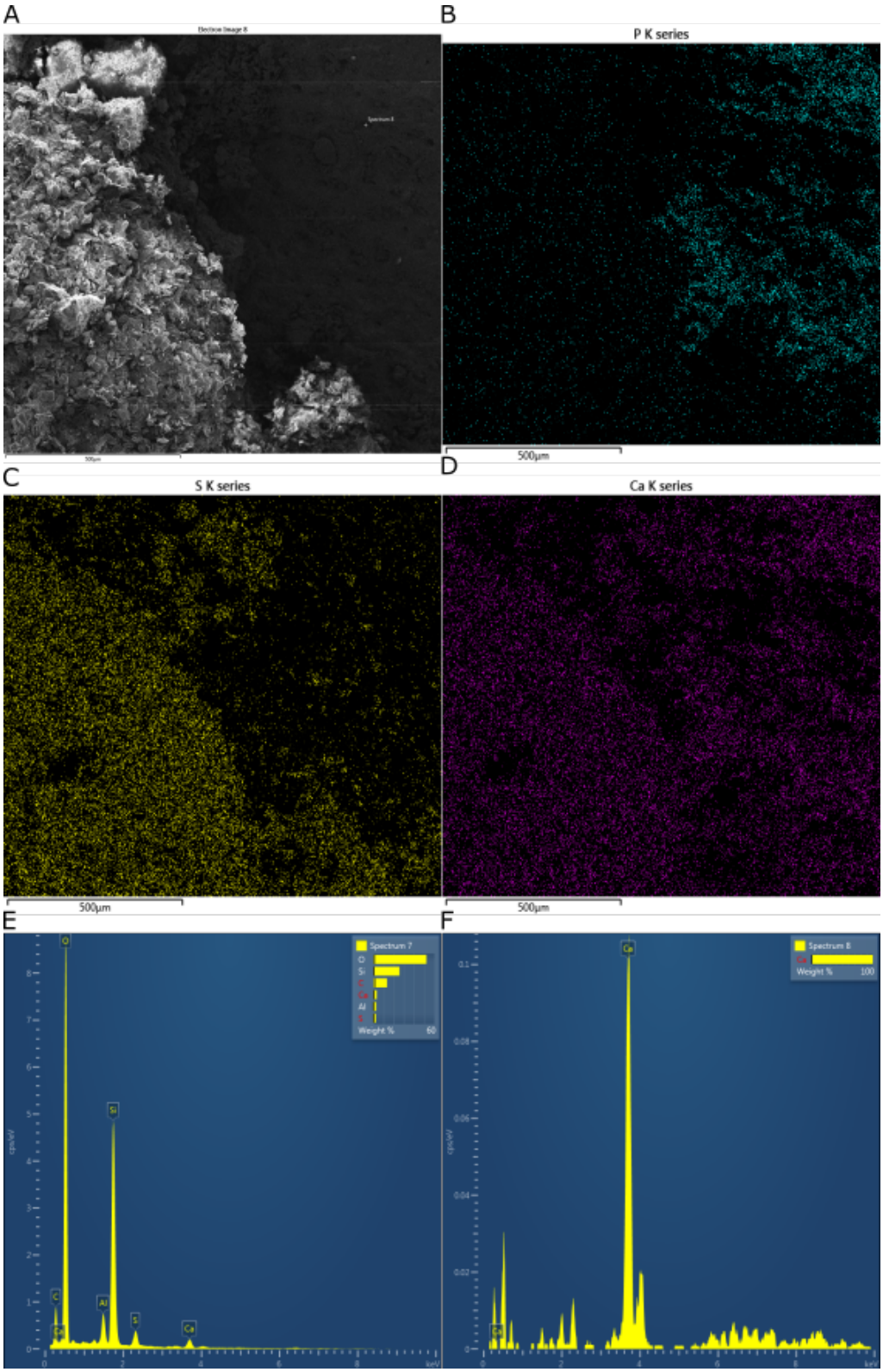

Figure 9: (a) Close up SEM image of the white coating on sample S_1. (b, c, d) EDS elemental maps for P, S and Ca. (e, f) Elemental spectra for points annotated in the SEM image.

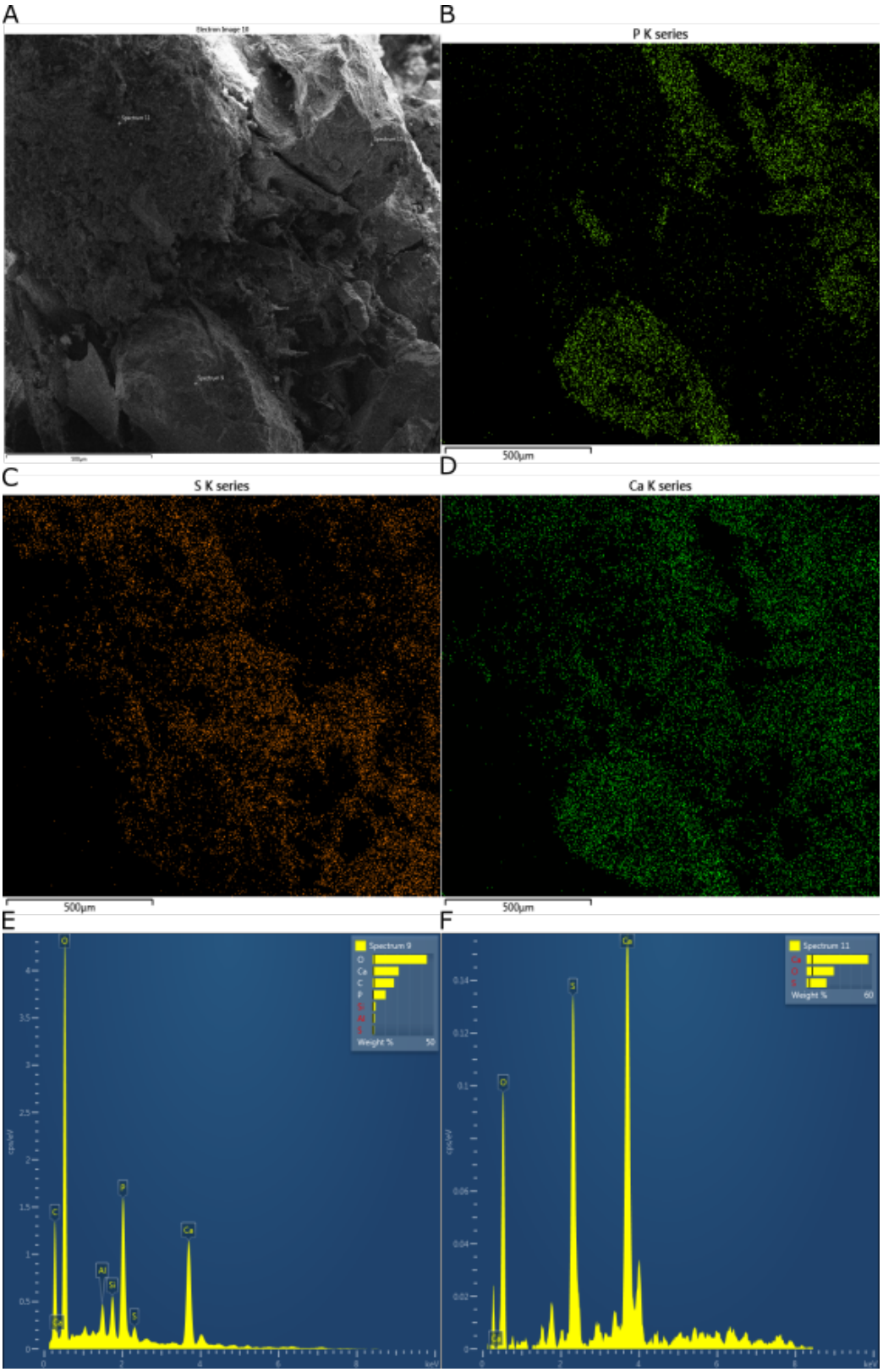

Figure 10: (a) Percentage of bones coated with any material based on unit in Blanche Cave Chamber 1. (b) Relative abundances of different coatings based on unit.

The coatings have varying levels of visibility under the SEM microscope. Black coatings are unseen, as the entire right half of the view is stained in black for Mn_3 [Figure 8]. On the other hand, white powdery coatings are very clear under the SEM [Figure 9]. While there is a difference in texture between the crystalline and bone material in C_1 [Figure 10], the interconnected nature of the mineral in the spongy bone makes it difficult to differentiate without the elemental map.

The EDS results produced elemental maps for the selected areas as well as spectra from specific points. The maps show counts of the specific element in the selected area and the spectra give relative concentrations of each element at that point. Manganese is present in bones that had a black coating but was not detected in any of the other bones [Figure 8]. The bones with the black coating also have manganese scattered on visually clean bone. The point scan spectra show a relatively higher concentration of manganese on the coated surface (~15 wt%, second most abundant) compared to the clean bone (undetected) [Figure 8]. Both phosphorus and sulphur are more restricted to their respective coatings, sulphur with the white powdery coating [Figure 9] and phosphorus with the crystalline coating [Figure 10]. The point scan for the white coating shows that it contains sulphur (>5 wt%, 6th most abundant) while clean bone has none [Figure 9]. The crystalline coating contains 10 wt% phosphorus (4th most abundant), but bone has no phosphorus detected [Figure 10]. These elements are also present in bones without those coatings, but in all cases, the zones they occupy do not overlap.

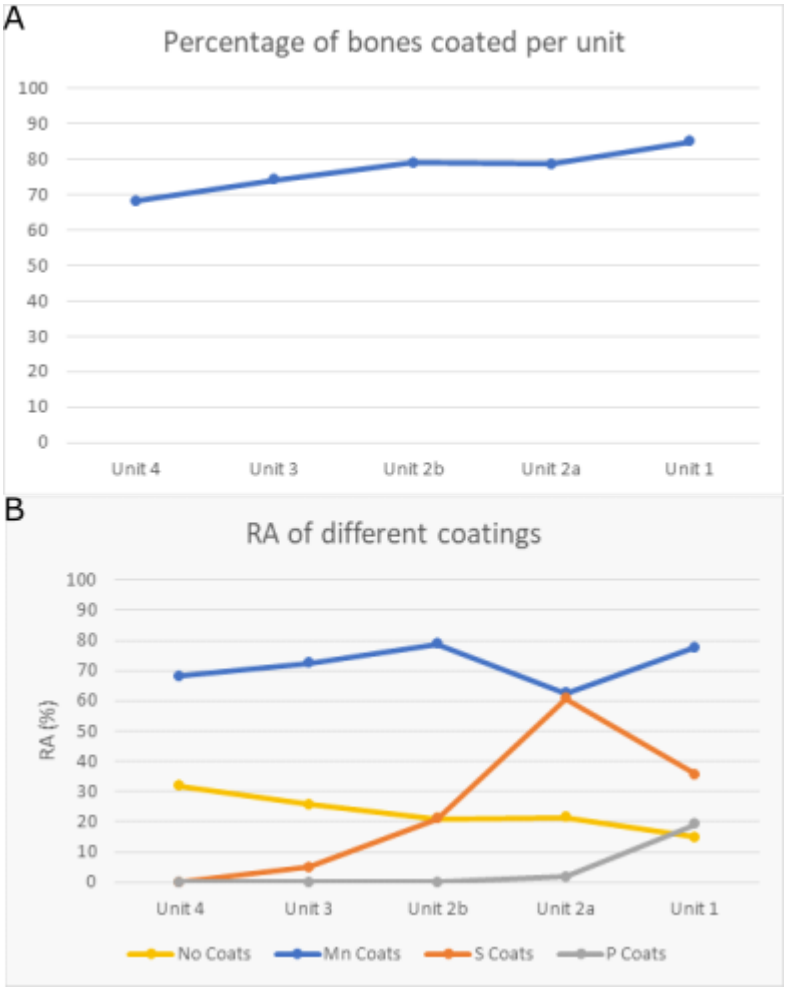

Figure 11: (a) Percentage of bones coated with any material based on unit in Blanche Cave Chamber 1. (b) Relative abundances of different coatings based on unit.

The relative proportion of bones that are coated per unit increases with depth from 68% at Unit 4 to 85% at Unit 1 [Figure 11]. Manganese coats are the most common, averaging at 72% and appear throughout the entire sequence [Figure 11]. White coats are second most abundant with an average of 30.5% and begin to appear at Unit 3, peaking at Unit 2a coating almost 60% of all bones. The crystals are the least common and restricted to the lowest units, with less than 5% at Unit 2a.

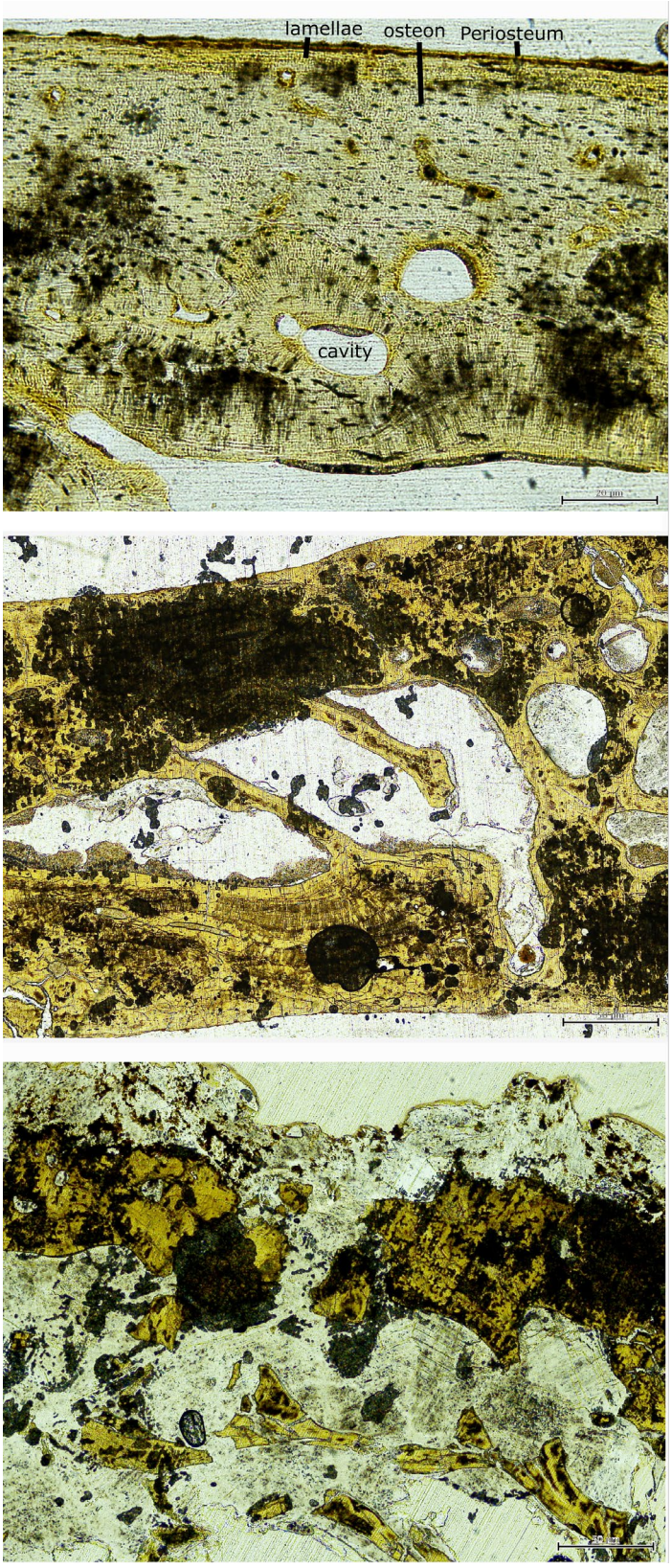

Figure 12: Thin section images of varying crystalline coating intensities on bone. (a) Is a sample that had no visible coatings, (b) is a sample that has some surface coatings, and (c) is a sample that is extensively coated.

Thin sections reveal three materials associated with the bone matrix. Bone material has a golden-brown colour with textural features present, however these features begin to disappear in more coated elements as the cracks are more common [Figure 12]. Present in all 3 bones is an opaque black material that can extend from below the bone surface to the centre of the bone. In slightly coated and very coated bones, a grainy mineral can be seen in bone canals and on remnants of bone [Figure 12]. In the very coated element, a colourless white mineral dominates the assemblage. In some places, the mineral appears to be replacing bone. While not as extensive, this same mineral is present in some canals of the slightly altered sample.

DISCUSSION

Sedimentology and geochronology

This site contains a 'classic' late Pleistocene sequence of dark reddish silts containing megafaunal material overlain by brown silty sand characteristic of LGM age deposits, topped by Holocene greyish sands (Forbes & Bestland, 2007). This general sequence of units is also present at the chamber 3 site (Darrénougué et al., 2009; Laslett, 2006) and other caves in the region (Macken et al., 2013a). What separates this site from that of the third chamber is the well-preserved laminations in Unit 2, as the corresponding unit in the chamber 3 pit does not have these sedimentary features.

The entire sequence has mostly horizontal boundaries between units with the exception of Units 5 and 6 [Figure 4], suggesting that it is relatively far from the sediment cone. Planar beds of coarser sand in Units 2a and 4 indicate a higher energy mode of deposition, with each sand bed marking a flow event. The well sorted undifferentiated

Units 2b and 3 could also represent mass dumping events that lead to high sedimentation rates. It is likely that these events involved some form of water flow to move this amount of sediment. There is a general increase in grain size through time, as younger units tend to be sandier compared to older units, suggesting a relative increase in energy of deposition for these units. The large channel disruption, along with its associated cut and fill structures, is also evidence for water action in the site.

The white material in Unit 1 is likely to be authigenic gypsum that formed due to changes in the surface soil environment. XRD analysis of this material confirms it to be predominantly gypsum with sub-dominant quartz (Appendix E). Authigenesis is a surface process, creating a pattern that traces past sediment floors and does not disrupt unit boundaries, as seen in the site [Figure 4]. In a cave environment, pooling of water collects sulphide ions which can precipitate gypsum (Yonge & Krouse, 1987). However, bat activity is the more likely cause as the chamber morphology and environment is preferred for wintering caves. The chamber has domed features on its ceiling [Figure 3], which is preferred by bats as they help retain heat released by endothermic activity (Baudinette et al., 1994). Bats have also been residing in other parts of the cave, as the cave is recorded to have an average temperature of 9-15C, which is in range of optimal wintering cave temperatures (Sanderson & Bourne, 2002). The bulk geochemistry for the white region of Unit 1 matches previous findings by Forbes and Bestland (2006) of having lower SiO_2, higher SO_3, CaO, P_2O_5 and LOI as a guano derived sediment [Table 1].

The gypsum nodules also have interesting structures within Unit 1 and in Units 2 and 3. In Unit 1, the gypsum is only found in certain zones, showing that the effect of bat guano on forming these minerals is localised. The bowl-shaped feature in unit 1 of the north face of the pit could easily be a cut and fill structure, but the unit is undisturbed, and the feature is more likely due to different geochemical conditions in the sediment. Since bats do not create uniform, spread-out guano deposits, guano must have not been dropped in that spot after a certain point. However, in this 'empty' zone are much larger (~2cm) nodules of the same material. This could suggest that the conditions for that portion of the unit favoured the formation of fewer, larger gypsum nodules, compared to many, small ones. Another interpretation of this feature could be a small pool of water that increased moisture in the surrounding sediment and dissolved gypsum in that region. Other unique features on the north wall are zones of gypsum incorporated sediment in Units 2 and 3. These zones extend only from large gypsum concentrations (in Unit 1 and in the channel structure) and can represent a gradient in the sediment due to leaching of elements from its sources (Yonge & Krouse, 1987) or zones of varying dryness.

Faunal Succession

Based on the relationships between higher animal groups [Figure 5], the shift from a marsupial to a placental dominated assemblage suggests a change in cave structure to a more open cave. This is different from chamber 3 where rodents are the most abundant group throughout the sequence (Laslett, 2006). The increased density of smaller animals along with acid etching of bone elements are characteristics of owl accumulation (Andrews, 1990). While owl assemblages are not uncommon at Naracoorte (Fraser &

Wells, 2006; Macken et al., 2012; Macken & Reed, 2013), the patterns seen could simply be an effect of having a small sample size.

Majority of the bat specimens occur in Unit 1, which is still reasonable as wintering cave assemblages do not contain as much bat material compared to maternity caves (Reed, pers. comm.). This supports the theory that bat activity has moved from the first to the third chamber. While the cave must have been getting more and more closed as sediment comes in, the shift to owl assemblages suggests a change towards a more open cave environment. This seems contradictory, but it is more likely that the change reflects the main chamber 1 conditions rather than specifically for this site. The relatively high energy deposition, water action, and estimated distance from the sediment cone supports the idea that material from the larger main chamber would have been washed into this small side chamber. What could have then happened was the movement of bats to a different part of the cave as this small chamber filled up, while opening of the main chamber changed the type of assemblage that would have washed in. This means that the site can be used to infer structural changes in the main chamber.

Like the Third Chamber site, megafaunal genera has been restricted to the lowest units [Figure 6]. While most of the megafaunal groups are concentrated in Unit 1, some isolated bones were located at the base of Unit 2. These isolated elements can represent disarticulation before entering the chamber and transport lag from the main chamber 1 to its current position. The variations in different murid groups towards the last glacial maximum (Unit 4) show the effects of climate on small mammals. Range expansion and contraction of different species due to climate change is likely since some of these

species are extinct (*P. gouldii*) or no longer live in the area (*M. fuscus*). The two species that show an increase towards Unit 4 (trend 1) have current habitats in grass and shrubland with dense vegetation, while those that have trend 3 (decrease towards Unit 4) prefer more open habitats. This suggests an increase in low vegetation and ground cover during the LGM.

The whole faunal assemblage of the site is also similar to the Third Chamber assemblage, having the same major groups of animals (Laslett, 2006). However, there are some groups present in this chamber that are absent in chamber three and vice versa [Table 3]. This site contains devil and wombat material, as well as one element from the extinct kangaroo *P. oscillans*. Because the unique species have counterparts with similar lifestyles and body sizes between the two sites, it can be hypothesized that the cave entrances and accumulation modes would be the same for both assemblages.

One caveat to these interpretations is that the depths of the fossil material relative to the different sedimentary units is estimated. Since the original data available from the 2001 excavation did not accurately record this information, an accurate, quantitative faunal succession analysis could not be done. However, the estimation should provide a good image of the actual succession since the units between this site and the Third chamber site are near identical and the chronology for that site may be used as a proxy. Another issue is that nothing labelled at 40-50cm depth was found, which can contain a significant portion of material. Since it is impossible for no bones to have been deposited at this interval, its absence in the data can skew results and interpretations.

Taphonomy of surface coatings

BLACK COATING

The black coatings are most likely to be due to manganese staining and not from burning. The bone surface stained in black has shown to be relatively abundant in manganese [Figure 8]. Furthermore, there is a lack of cracking, flaking and calcination that is caused by burning (Fernández-Jalvo et al., 2018). Some of the stains have a shiny, sometimes slightly blue hue to it, which are characteristic of a manganese coat. While inorganic oxidation of manganese is possible, it is kinetically inhibited even with high concentrations of Mn (Carmichael & Brauer, 2015).

The coating mechanism for manganese is different from the other two coatings since the element is not restricted to just the observed stain [Figure 8]. The manganese penetrates the bone surface with some reaching the centre of the bone [Figure 12], similar to those studied by Hollund et al. (2018). This is likely due to the manganese being absorbed by the bone while inundated, which is later oxidized by bacteria to form the coats. The dendritic features of some coatings support the involvement of bacteria in this process (Papier et al., 2011). Multiple studies have suggested the oxidation of different ions as a potential source of energy for microorganisms in the absence of light in a process called chemolithotrophy (Carmichael and Brauer, 2015; Kotula et al., 2019; Papier et al., 2011). Dissolved manganese in cave waters could come from the carbonate bedrock itself (López-González et al., 2006), as the ion easily substitutes for Ca^{2+} in the mineral structure. Mn requires an acidic, reducing environment to reside in solution, which is created by decomposing organic matter. The bacteria that oxidize the ions work

optimally at a higher pH but are stimulated by carbon influx (Carmichael and Brauer, 2015) and H_2SO_4 (Kotula et al., 2019), which are both supplied by decaying guano.

While inundation of the bone surface was theorised for manganese to concentrate and be absorbed into the bone, this does not seem to be a requirement as black coatings are present throughout the sequence regardless of evidence for pooling of water in the cave. Since oxidation of Mn indicates an aerated, sometimes dry, environment (Hollund et al., 2019), as long as there is a pathway for Mn ions to enter the bone, subsequent oxidation and staining can occur. Therefore, the presence of manganese coatings does not necessarily indicate pooling of water, but instead informs us of the amount of moisture in its microenvironments. However, the fact that some bones in the same unit have zero or undetectable manganese levels on its surface suggests that these conditions can be very localised within the soil environment, making it an unreliable proxy for larger scale reconstructions.

WHITE POWDERY COATING

The white powdery coating looks very similar to the nodules found in the older units of the sequence and has relatively high amounts of sulphur [Figure 9], suggesting this is the same gypsum that is coating the bone. The material does not seem to incorporate itself and get absorbed into the bone [Figure 13], and the sulphur is restricted mainly to the coatings based on the elemental maps. This means that the bone surface is only used as a substrate for it to grow on. Like manganese, oxidation by bacteria has also been suggested as an important step in the formation process (Dumitras et al., 2008; Shahack-Gross et al., 2004). Leaching guano produces substantial concentrations of sulphur ions,

which are oxidized to sulphuric acid (Shahack-Gross et al., 2004). Ca is then sourced from the host rock or cave waters that interact with the sulphuric acid (Audra et al., 2019). Since gypsum is a easily dissolvable hydrated mineral, it indicates an initial wet acidic environment that dries up to preserve the coating.

Gypsum coatings start to appear at Unit 3 and peak at Unit 2a [Figure 11]; however, these units do not have extensive incorporation of the nodules in the sediment as in Unit 1. Suggesting that there must be something about the bone that promotes mineralisation since it is coating the bone, but not forming on its own in the surrounding sediment. This might be since bacteria would rather concentrate near organic matter as it provides them with resources. Another possible reason could be that the bone has a different pH compared to the sediment around it, making it a better substrate for growth. The presence of gypsum in Unit 1 could then indicate an even higher amount of sulphur in the sediment for it to form on bone and as isolated nodules.

However, due to the lack of information from original field notes, all of the coated bones could have come from zones of gypsum in units 2 and 3, which would mean that gypsum coating is restricted to microenvironments where it is stable.

CRYSTALLINE COATING

The third mineral appears to be compromising the bone rather than simply coating the surface. Under the SEM, the material contains high amounts of phosphorus with little to no sulphur while the unaffected areas around it shows the opposite trend [Figure 10]. This indicates that it is unlikely to be gypsum and is some type of phosphate mineral

that forms on/in the bone. The degradation of bone material due to bat guano has been recorded in archaeological studies to show that assemblages can be biased by this phenomenon (Shahack-Gross et al., 2004). The same study has shown that bat guano, along with microorganisms that decompose it, alter soil chemistry by decreasing the pH. The altered bone, if in close contact with the remaining phosphate, could then recrystallize as a different mineral. This explains why an extensively coated element [Figure 12] has very few bone structures left with most of it being coating.

The main source of phosphate is presumed to be from bat guano after the mobile nitrate component of guano leaches out (Shahack-Gross et al., 2004). While this can be the case for fossil guano deposits (Dumitras et al., 2008), since the crystals are not found on their own in the sediment it is likely that the phosphate source is bone hydroxyapatite. By degrading the bone, the liberated phosphate can be oxidized to form the coatings. This can explain why coatings under thin section appear where bone should be and forming within cracks in the bone as the bacteria are using the substrate as a source [Figure 12].

Like guano-derived minerals, the coating requires bones to be on the surface for an extended amount of time for guano and/or urine to be able to land on and dissolve them. The bones could not have been washed into the site by water immediately since the water would be slightly alkaline due to incorporation of carbonates from the cave and neutralize the pH. This sequence of events is possible since apatite, which is the most common guano derived phosphate, crystallizes at slightly acidic to neutral pH while more acidic (5.7-6.1 pH) environments promotes formation of taranakite instead (Audra

et al., 2019; Dumitras et al., 2008; Wurster et al., 2015). However, once the bone structure has been compromised, flow events can later affect what type of mineral begins to form. The other effect of requiring direct contact would mean that the extent of this coating would be the most restricted of all three coatings studied. This type of preservation is seen in Bat Cave, where very damaged material is next to well preserved bone, with the destroyed element being subject to constant drip water (Reed, pers. comm.). This supports the other lines of evidence that suggest bats using this section of the cave moved after Unit 2 was deposited.

Implications

The Chamber 1 excavation provides a strong case for comparing multiple sites in palaeontological studies. The sedimentary sequence found here matches those found in other synchronous deposits, with some minor variations in specific units. With a more resolved geochronology, palaeoclimate proxies from the site can be used to strengthen past climate reconstructions and identify factors that affect sediment accumulation between sites. For example, the unit that correlates to Unit 2a in Chamber 3 does not have laminations even if the cave entrances are close (~100 m) to each other. Factors such as having a smaller entrance size and increased distance from the accumulation point could lead to more punctuated, smaller flow events, as opposed to a mass dump. The presence of the rare *P. oscillans* in this site shows how having a small sample size can lose parts of a faunal assemblage, further highlighting the value of having multiple replicates.

While the exact ages of the coatings are unable to be calculated, this thesis provides some useful insights in the timing of their formation. Most degradation of bone (e.g.

acidic conditions from leaching guano and/or urine, cracking from alternating wet and dry conditions) would occur on the surface as it is more difficult to destroy bone once it has been buried. Manganese ions can enter the bone structure if partial inundation occurs at this stage. Phosphate and gypsum coatings form while the bone is still on the surface, similar to a fossil guano deposit. Guano-derived coatings form on relatively fast timescales (decades) and begin almost immediately (Shahack-Gross et al., 2004). Throughout the deposition and burial of fossil bone, chemolithotrophic bacteria are oxidizing ions as part of the coating process.

CONCLUSIONS

The overarching aim of this thesis was to conduct a chronostratigraphic, geochemical, and faunal analysis of a site in Blanche Cave Chamber 1. The results obtained have shown that the deposit shares the same characteristics with Chamber 3 and other Late Pleistocene sites at NCNP, having the three general sediment types with structures and accessory minerals that form due to site-specific depositional events and conditions. From a faunal perspective, the first chamber assemblage is similar to other Late Pleistocene to Holocene NCNP sites, sharing 80 percent of its species with other assemblages and having megafaunal material restricted to the dark red sandy clay layer. Its value as a replicate is in its addition of *Sarcophilus* and *Vombatidae* data to Blanche Cave and, more importantly, another *P. oscillans* element to the Naracoorte dataset.

Three fossil bone surface coatings present in this site and others in the NCNP have been identified. Mechanisms for the formation of these coatings have been proposed which allows us to infer the burial conditions of these bones. Manganese oxide stains require wet anoxic conditions for ions in solution to enter inundated bone, followed by slightly

acidic (5.5 to 6 pH) aerated environments for bacterial oxidation to occur. Gypsum coatings form in similar conditions as authigenic gypsum, suggesting an initial wet acidic environment followed by dry conditions to prevent the mineral from dissolving. Phosphates, such as hydroxyapatite, can replace bone material after the structure has been compromised by guano and form from biologic oxidation of phosphates, crystallizing at a slightly higher pH (6-7). In all three cases, guano and chemolithotrophic microorganisms play a key role in the early diagenetic processes that can occur on fossil bone and sediment substrate.

The site is very promising as there is still at least a meter of sediment left to excavate. Furthermore, better records of exact positions of coated elements can reveal the actual ranges of the burial microenvironments. As bone acts as an open system which closes once mineralization is complete, REE concentrations can fingerprint specific elements to units (Trueman et al., 2008). This can be used to better place the material to their proper depth. Other studies on bone REEs have used them as palaeoclimate proxies (Li et al. 2018), suggesting the possibility of REEs as a proxy for cave environments. Using authigenic minerals found in cave sequences to form mineral stability fields could also disentangle different cave processes and factors which control the burial environment.

More geochronologic work must be done on the site, as there are only two dates for the entire sequence. Bone samples for radiocarbon were collected during this study, but dates were not able to be obtained in time. Optically Stimulated Luminescence is also needed for the lower units as it is past the effective age range of radiocarbon dating.

Better characterization of the different coatings is needed. Guano derived deposits can form a suite of different minerals, each with their own stable conditions (Audra et al., 2019; Snow et al., 2014). Quantitatively identifying coatings recovered from bones using XRD will give a more accurate picture of burial conditions. Similar to a 'disarticulation sequence' for bone elements (Reed, 2001), a rank order of disintegration could be used to determine which elements tend to get chemically destroyed first to use phosphate coatings to determine what is missing from an assemblage.

ACKNOWLEDGMENTS

I would like to thank my supervisors, Liz Reed and Lee Arnold, for the support and feedback they have provided throughout my project, Derrick Hasterok and Katie Howard for managing the first mid-year honours cohort for geology, the other mid-year guinea pigs for moral support, Adelaide Microscopy for training and use of the SEM, Adelaide Petrography for cutting thin-sections and Bureau Veritas for geochemical analyses. I would also like to acknowledge Steve Brown for providing field notes, Naracoorte Caves staff for support, Mary-Anne Binnie for access and assistance with the SAM palaeontology collection. Funding for this project was under ARC Linkage project LP160101249 and research partners Department of Environment and Water, Naracoorte Lucindale Council, SA Museum, Terre a Terre, Wrattonbully Wine Industries Association, Defence Science and Technology Group.

REFERENCES

ANDREWS, P. (1990). *Owls, Caves and Fossils*. Chicago: University of Chicago Press.

AUDRA, P., DE WAELE, J., BENTALEB, I., CHROŇÁKOVÁ, A., VACLAV, K., D'ANGELI, I., . . . SANZ ARRANZ, A. (2019). Guano-related phosphate-rich minerals in European caves. *International Journal of Speleology, 48*, 75-105. doi:10.5038/1827-806X.48.1.2252

BAUDINETTE, R. V., WELLS, R., SANDERSON, K., & CLARK, B. (1994). Microclimatic Conditions in Maternity Caves of the Bent-wing Bat, Miniopterus schreibersii: an Attempted Restoration of a former Maternity Site. *Wild. Res., 21*, 607-619.

BROWN, S. (2006). ABSTRACTS FROM CAVEPS 2005. *Alcheringa: An Australasian Journal of Palaeontology, 30*(sup1), 429-475. doi:10.1080/03115510609506876

CARMICHAEL, S. K., & BRÄUER, S. (2015). Microbial diversity and manganese cycling: a review of Mn-oxidizing microbial cave communities. In A. S. Engel (Ed.), *Microbial Life of Cave Systems* (pp. 137-160). Boston, MA: De Gruyter.

DARRÉNOUGUÉ, N., DE DECKKER, P., FITZSIMMONS, K. E., NORMAN, M. D., REED, L., VAN DER KAARS, S., & FALLON, S. (2009). A late Pleistocene record of aeolian sedimentation in Blanche Cave, Naracoorte, South Australia. *Quaternary Science Reviews, 28*(25), 2600-2615. doi:https://doi.org/10.1016/j.quascirev.2009.05.021

DUMITRAS, D., HATERT, F., BILAI, E., & MARINCEA, S. (2004). Gypsum and bassanite in the bat guano deposit from the « dry » Cioclovina cave (Sureanu Mountains, Romania). *Romanian Journal of Mineral Deposits, 81*, 3.

EASTON, L. C. (2006). Pleistocene Grey Kangaroos from the Fossil Chamber of Victoria Fossil Cave, Naracoorte, South Australia. Transactions of the Royal Society of South Australia, 130, 17-28.

FERNÁNDEZ-JALVO, Y., TORMO, L., ANDREWS, P., & MARIN-MONFORT, M. D. (2018). Taphonomy of burnt bones from Wonderwerk Cave (South Africa). *Quaternary International, 495*, 19-29. doi:https://doi.org/10.1016/j.quaint.2018.05.028

FIELD, J., FILLIOS, M., & WROE, S. (2008). Chronological overlap between humans and megafauna in Sahul (Pleistocene Australia–New Guinea): A review of the evidence. *Earth-Science Reviews, 89*(3), 97-115. doi:https://doi.org/10.1016/j.earscirev.2008.04.006

FOECKE, K. (2016). *SURFACE MICROANALYSIS OF STAINING ON VERTEBRATE FOSSIL BONE FROM THE SANTA FE RIVER, FLORIDA* (Master of Science), Pennsylvania State University.

FORBES, M., & BESTLAND, E. (2006). Guano-derived deposits within the sandy cave fills of Naracoorte, South Australia. *Alcheringa: An Australasian Journal of Palaeontology, 30*, 129-146. doi:10.1080/03115510609506859

FORBES, M., & BESTLAND, E. (2007). Origin of the sedimentary deposits of the Naracoorte Caves, South Australia. *Geomorphology, 86*. doi:10.1016/j.geomorph.2006.09.009

FRASER, R., & WELLS, R. (2006). Palaeontological excavation and taphonomic investigation of the late Pleistocene fossil deposit in Grant Hall, Victoria Fossil Cave, Naracoorte, South Australia. *Alcheringa: An Australasian Journal of Palaeontology, 30*, 147-161. doi:10.1080/03115510609506860

GILLESPIE, R. (2008). Updating Martin's global extinction model. *Quaternary Science Reviews, 27*(27), 2522-2529. doi:https://doi.org/10.1016/j.quascirev.2008.09.007

HILL, A., & BEHRENSMEYER, A. (1984). Disarticulation Patterns of Some Modern East African Mammals. *Paleobiology, 10*, 366-376. doi:10.1017/S0094837300008332

HILL, C. A. (1982). Origin of Black Deposits in Caves. *Quarterly Journal of The National Speleological Society, 44*(1), 4.

HOLLUND, H., BLANK, M., & SJÖGREN, K.-G. (2018). Dead and buried? Variation in post-mortem histories revealed through histotaphonomic characterisation of human bone from megalithic graves in Sweden. *PLOS ONE, 13*, e0204662. doi:10.1371/journal.pone.0204662

KARKANAS, P., BAR-YOSEF, O., GOLDBERG, P., & WEINER, S. (2000). Diagenesis in Prehistoric Caves: the Use of Minerals that Form In Situ to Assess the Completeness of the Archaeological Record. *Journal of Archaeological Science, 27*(10), 915-929. doi:https://doi.org/10.1006/jasc.1999.0506

KOTULA, P., ANDREYCHOUK, V., PAWLYTA, J., MARYNOWSKI, L., & JENDRZEJEWSKA, I. (2019). Genesis of iron and manganese sediments in Zoloushka Cave (Ukraine/Moldova) as revealed by δ13C organic carbon. *IJS, 48*(3).

LASLETT, T. M. (2006). *A Palaeoecological Study of a Quaternary Vertebrate Fossil Deposit in Blanche Cave, Naracoorte, South Australia* (Honours in BSc Biodiversity and Conservation), Flinders University.

LI, M., OUYANG, T., ZHU, Z., TIAN, C., PENG, S., TANG, Z., . . . PENG, X. (2019). Rare earth element fractionations of the northwestern South China Sea sediments, and their implications for East Asian monsoon reconstruction during the last 36 kyr. *Quaternary International, 525*, 16-24. doi:https://doi.org/10.1016/j.quaint.2019.09.007

LÓPEZ-GONZÁLEZ, F., GRANDAL-D'ANGLADE, A., & VIDAL-ROMANI, J. R. (2006). Deciphering bone depositional sequences in caves through the study of manganese coatings. *Journal of Archaeological Science, 20*, 707-717. doi:10.1016/j.jas.2005.10.006

MACKEN, A., PRIDEAUX, G., & REED, E. (2012). Variation and pattern in the responses of mammal faunas to Late Pleistocene climatic change in southeastern South Australia. *Journal of Quaternary Science, 27*, 415-424. doi:10.1002/jqs.1563

MACKEN, A., MCDOWELL, M., BARTHOLOMEUSZ, D., & REED, E. (2013). Chronology and stratigraphy of the Wet Cave vertebrate fossil deposit, Naracoorte, and relationship to paleoclimatic conditions of the Last Glacial Cycle in south-eastern Australia. *Australian Journal of Earth Sciences, 60*, 271-281. doi:10.1080/08120099.2013.758657

MACKEN, A., & REED, E. (2013). Late Quaternary small mammal faunas of the Naracoorte Caves World Heritage Area. *Transactions of the Royal Society of South Australia, Incorporated: incorporating the records of the South Australian Museum, 137*, 53-67.

MACKEN, A. C., STAFF, R. A., & REED, E. H. (2013). Bayesian age-depth modelling of Late Quaternary deposits from Wet and Blanche Caves, Naracoorte, South Australia: A framework for comparative faunal analyses. *Quaternary Geochronology, 17*, 26-43. doi:https://doi.org/10.1016/j.quageo.2013.03.001

MARÍN ARROYO, A. B., LANDETE RUIZ, M. D., VIDAL BERNABEU, G., SEVA ROMÁN, R., GONZÁLEZ MORALES, M. R., & STRAUS, L. G. (2008). Archaeological implications of human-derived manganese coatings: a study of blackened bones in El Mirón Cave, Cantabrian Spain. *Journal of Archaeological Science, 35*(3), 801-813. doi:https://doi.org/10.1016/j.jas.2007.06.007

PAPIER, S., BAELE, J.-M., GILLAN, D., BARRIQUAND, L., & BARRIQUAND, J. (2011). MANGANESE GEOMICROBIOLOGY OF THE BLACK DEPOSITS FROM THE AZÉ CAVE, SAÔNE-ET-LOIRE, FRANCE. *Quaternaire, 4*, 297-305.

PRICE, G., LOUYS, J., SMITH, G., & CRAMB, J. (2019). Shifting faunal baselines through the Quaternary revealed by cave fossils of eastern Australia. *PeerJ, 6*, e6099. doi:10.7717/peerj.6099

PRIDEAUX, G. J., ROBERTS, R. G., MEGIRIAN, D., WESTAWAY, K. E., HELLSTROM, J. C., & OLLEY, J. M. (2007). Mammalian responses to Pleistocene climate change in southeastern Australia. *Geology, 35*(1), 33-36. doi:10.1130/G23070A.1

REED, E. (2001). Disarticulation of kangaroo skeletons in semi-arid Australia. *Australian Journal of Zoology, 49*, 615-632. doi:10.1071/ZO01010

REED, E. (2006). In Situ Taphonomic Investigation of Pleistocene Large Mammal Bone Deposits from The Ossuaries, Victoria Fossil Cave, Naracoorte, South Australia. *Helictite, 39*, 5-15.

REED, E. H., & BOURNE, S. J. (2000). Pleistocene fossil vertebrate sites of the South East region of South Australia. *Transactions of the Royal Society of South Australia, Incorporated., 124*, 61-90.

REED, E. H., & BOURNE, S. J. (2009). Pleistocene Fossil vertebrate Sites of the South East Region of South Australia II. *Transactions of the Royal Society of South Australia, 133*(1), 30-40. doi:10.1080/03721426.2009.10887108

ROBERTS, R. G., FLANNERY, T. F., AYLIFFE, L. K., YOSHIDA, H., OLLEY, J. M., PRIDEAUX, G. J., . . . SMITH, B. L. (2001). New Ages for the Last Australian Megafauna: Continent-Wide Extinction About 46,000 Years Ago. *Science, 292*(5523), 1888. doi:10.1126/science.1060264

SALTRÉ, F., RODRÍGUEZ-REY, M., BROOK, B. W., JOHNSON, C. N., TURNEY, C. S. M., ALROY, J., . . . BRADSHAW, C. J. A. (2016). Climate change not to blame for late Quaternary megafauna extinctions in Australia. *Nature communications, 7*, 10511-10511. doi:10.1038/ncomms10511

SANDERSON, K., & BOURNE, S. (2002). Cave Temperatures at Naracoorte Caves. *Helictite, 38*, 7-10.

SHAHACK-GROSS, R., BAR-YOSEF, O., & WEINER, S. (1997). Black-Coloured Bones in Hayonim Cave, Israel: Differentiating Between Burning and Oxide Staining. *Journal of Archaeological Science, 24*, 439–446. doi:10.1006/jasc.1996.0128

SHAHACK-GROSS, R., BERNA, F., KARKANAS, P., & WEINER, S. (2004). Bat guano and preservation of archaeological remains in cave sites. *Journal of Archaeological Science, 31*, 1259-1272. doi:10.1016/j.jas.2004.02.004

SNOW, M., PRING, A., & ALLEN, N. (2014). Minerals of the Wooltana Cave, Flinders Ranges, South Australia. *Transactions of the Royal Society of South Australia, 138*. doi:10.1080/03721426.2014.11649009

STATHOPOULOU, E., PHOCA COSMETATOU, N., THEODOROPOULOU, T., MALLOUCHOU, M., MARGARITI, E., & PSYCHARIS, V. (2019). Origin of archaeological black bones within a waterlogged context: A multidisciplinary approach. *Palaeogeography, Palaeoclimatology, Palaeoecology, 534*, 109334. doi:https://doi.org/10.1016/j.palaeo.2019.109334

TRUEMAN, C. N., PALMER, M. R., FIELD, J., PRIVAT, K., LUDGATE, N., CHAVAGNAC, V., . . . ROGERS, R. R. (2008). Comparing rates of recrystallisation and the potential for preservation of biomolecules from the distribution of trace elements in fossil bones. *Comptes Rendus Palevol, 7*(2), 145-158. doi:https://doi.org/10.1016/j.crpv.2008.02.006

WHITE, S., & WEBB, J. A. (2015). The influence of tectonics on flank margin cave formation on a passive continental margin: Naracoorte, Southeastern Australia. *Geomorphology, 229*, 58-72. doi:https://doi.org/10.1016/j.geomorph.2014.09.003

WURSTER, C. M., MUNKSGAARD, N., ZWART, C., & BIRD, M. (2015). The biogeochemistry of insectivorous cave guano: a case study from insular Southeast Asia. *Biogeochemistry, 124*(1), 163-175. doi:10.1007/s10533-015-0089-0

YONGE, C. J., & KROUSE, H. R. (1987). The origin of sulphates in Castleguard Cave, Columbia Icefields, Canada. *Chemical Geology: Isotope Geoscience section, 65*(3), 427-433. doi:https://doi.org/10.1016/0168-9622(87)90018-2

APPENDIX A: TABLE OF SEDIMENT SAMPLES

Sediment samples were collected during fieldwork for this study.

Cave	Unit	Sample #	# of vials	Grid	Wall	Depth (cm)	Notes
5U4	1	1	2	1	E	100	1 for comparative 1 for geochem (XRF)
5U4	1	2	2	2	E	970	1 for comparative 1 for geochem (XRF), has white stuff
5U4	2a	3	2	1	E	710	1 for comparative 1 for geochem (XRF)
5U4	2b	4	2	1	E	670	1 for comparative 1 for geochem (XRF)
5U4	3	5	2	4	N	750	1 for comparative 1 for geochem (XRF)
5U4	4	6	2	4	N	500	1 for comparative 1 for geochem (XRF)
5U4	5	7	2	4	N	350	1 for comparative 1 for geochem (XRF)
5U4	6	8	2	4	N	245	1 for comparative 1 for geochem (XRF), came from same hole
5U4	O/B	9	1	4	N	120	1 for comparative
5U4	1	10	3	4	N	1130	scraped larger nodules for XRD
5U4	1	11	2	4	N	~1200 -1600	scraped powdery white surface for XRD

APPENDIX B: XRD PROCEDURES AND SPECIFICATIONS

The samples were pulverised in a mortar and pestle and then lightly pressed into a back-packed sample holder. The XRD trace was collected under the following instrument conditions:

XRD generator	PANalytical X'Pert Pro PW3040 diffractometer, 40 kW, 40 mA
Filter	Iron
Radiation	CoKα (λ = 1.789Å)
Angular range	5° to 80° 2θ
Angular speed	0.04426° 2θ/second
Time per step	50.165
Step size	0.0167°
Divergence Slit	¼°
Anti-scatter Slit	½°
Spinning	4 seconds per revolution

APPENDIX C: SORTING PROCEDURES

All screening and sorting was conducted while wearing latex gloves to decrease carbon contamination. Leaves were removed prior to wet screening and kept in bags while sediment was collected in vials. Some small bone fragments were also in the vials as they were difficult to separate from the sediment. Material was wet screened by slight agitation in a sieve partially submerged in a bucket of water, making sure that the top of the sieve is never submerged in the water. Screened material was left to air dry in trays, as using paper towels could contaminate samples with carbon. Material was then sorted for cranial material (for identification and faunal succession analysis), speleothem fragments (for U-Pb dating), iron and phosphate nodules (for chemical analysis), and bone fragments with surface coatings. Samples for carbon dating were loosely wrapped in aluminium foil to prevent further contamination.

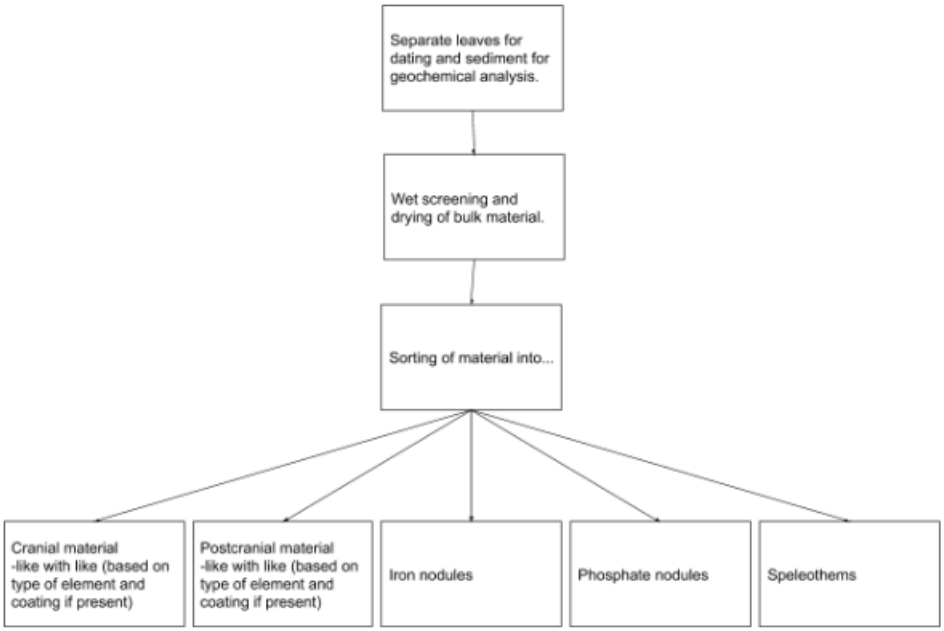

APPENDIX D: TABLE OF SAMPLES USED IN DESTRUCTIVE SAMPLING

Sample	Source/Sample #	Depth	Grid Square	Analysis
Mn_1	Bulk bag 54	70-80cm (Unit 1)	1	SEM-EDX
Mn_2	Bulk bag 54	70-80cm (Unit 1)	1	SEM-EDX
Mn_3	Bulk bag 54	70-80cm (Unit 1)	1	SEM-EDX
S_1	Bulk bag 54	70-80cm (Unit 1)	1	SEM-EDX
C_1	BCA 330	70-80cm (Unit 1)	4	SEM-EDX
	BCA 053	Overburden	Not specified	Thin sectioned
55-G4	Bulk bag 55	70-80cm (Unit 1)	4	Thin sectioned
	BCA 077	Overburden	Not specified	Thin sectioned
	Bulk bags 41, 39, 38	0-20cm (Units 4 & 3)	4	14C dating
	Bulk bag 50	30-40cm (Unit 2b)	4	14C dating
	Bulk bags 56, 57, 58	70-80cm (Unit 1)	4	14C dating

APPENDIX E: QUALITATIVE XRD RESULTS

Mineral	Composition	5U4:1: 10a	5U4:1: 10b	5U4:1: 10c	5U4:1: 11
Gypsum	$CaSO_4(H_2O)_2$	D	D	D	SD
Quartz	SiO_2	SD	A	SD	D
Amphibole group*	$A_{0-1}B_2Y_5Z_8O_{22}(OH, F, Cl)_2$	Tr	Tr	Tr	Tr
Unassigned peak*	Unknown	Tr			Tr

Amphibole group: Where A=Ca, Na, K, Pb; B=Ca, Fe2+, Li, Mg, Mn2+, Na; Y=Al, Cr3+, Fe2+, Fe3+, Mg, Mn2+, Ti, Z=Al, Be, Si. Magnesiohornblende was used in these QXRD refinements.
Due to the lack of other identifying peaks, a number of unidentified peaks/phases were observed. Further work is required to determine the mineral giving rise to this peak.

Tr = Trace. i.e. the mineral that gives rise to this peak is assumed to be present in trace amounts.
A = Accessory. Components judged to be present between the levels of roughly 5 and 20%.
SD = Sub-dominant. The next most abundant component(s) providing its percentage level is judged above about 20%.
D = Dominant. Used for the component apparently most abundant, regardless of its probable percentage level.